INTRODUCTION

Fluorescence is a form of emission spectroscopy that can provide information useful in qualitative and quantitative analysis. When one of the electrons of a molecule in the singlet state is excited by absorption of a photon, a singlet state is formed. In the excited singlet state, the spin of the promoted electron is still paired with the ground state electron. *Fluorescence*[1] can be produced when the emitted photons come from the excited singlet states (Figure-1). An excited singlet electron can be deactivated by fluorescence emission and by internal conversion or by external conversion.

It is important to note that few compounds exhibit fluorescence, because an electronically excited molecule ordinarily returns to the ground state by internal or external conversion.[1] The most intense and the most useful fluorescence is usually found in compounds containing aromatic functional groups, because these have large π systems that provide enough π orbitals to fluoresce.

Fluorescence is easily quenched by lone pairs of electrons,[2] as well as other mechanisms. A compound with fluorescent groups may not show fluorescent properties if it contains elements with lone pairs of electrons, especially nitrogen. Some metal ions can prevent the lone pair electrons from quenching the fluorescent groups by forming a coordinate bond with the lone pair electron donors. The ligand, 10-bis (TMEDA) anthracene is non-fluorescent when it is in aqueous solution alone (Figure-2). When the nitrogen forms a chelate ring with Zn^{2+}, the metal complex is over 1000-times more fluorescent than the free ligand.[3] This effect is referred to as the Chelation Enhanced Fluorescence (CHEF) effect.[4-9]

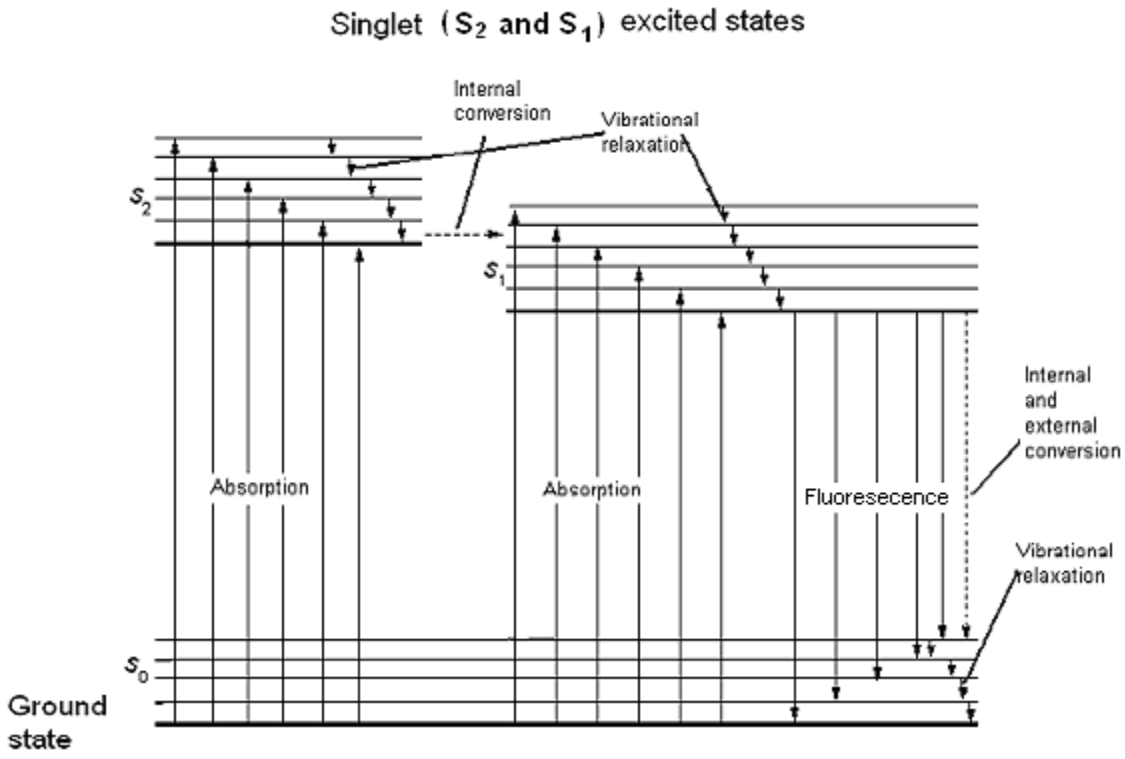

Figure-1. Partial energy diagram for a fluorescence system.[1]

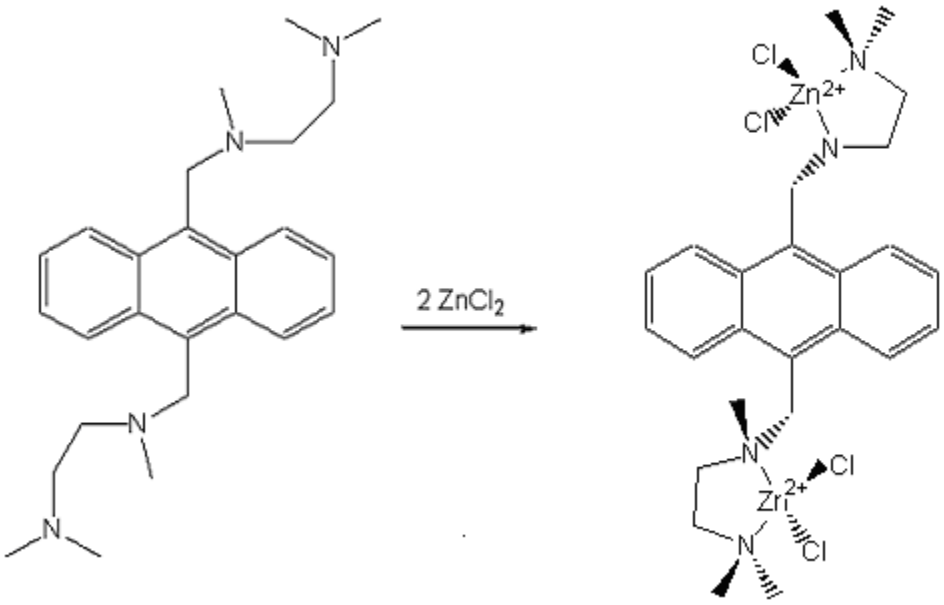

Figure-2. CHEF effect of Zn^{2+}-*bis* (TMEDA) anthracene ligand complex.[3]

Chelating ligands are compounds with more than one donor atom, which can form chelate rings when they form coordination complexes with metal ions (Figure-2). Unidentate ligands have one donor atom, such as $(CH_3)_3N$, OH^-, F^-. The increased stability produced when chelating ligands form coordination complexes with metal ions, compared with those of unidentate analogues, is known as the chelate effect. This is seen for the formation constants of the complexes of Ni^{2+} with *n*-dentate polyamines, as compared with the analogous complexes with ammonia (Table-1)[10]. The formation constants (log*K*) of n-dentate polyamines are much larger than the $\log\beta_n(NH_3)$. $\beta_n(NH_3)$ is the formation constant of Ni^{2+} with n number of ammonia ligands.

The widespread and important use of fluorescence indicators in the nondestructive monitoring of the activity or free concentrations of important ions or messengers employs the CHEF effect. An application of particular interest is the development of CHEF sensors for zinc in a low concentration system, such as nerve tissues.[4-9] Evidence suggests that zinc imbalances are involved in seizures that occur in epilepsy, neuro-degenerative diseases, and traumatic brain damage.[9]

Table-1. Chelate effect for complexes of Ni(II) with polyamines.[10]

polyamine	EN	DIEN	TRIEN	TETREN	PENTEN
denticity, n	2	3	4	5	6
log $\beta_n(NH)_3$	5.08	6.85	8.12	8.93	9.08
log K_1(polyamine)	7.47	10.07	14.4	17.4	19.1

Where:
Ionic strength = 0.5 *M*
Denticity means the number of binding ligands in one molecule.
EN $NH_2CH_2CH_2NH_2$
DIEN $NH_2(CH_2CH_2NH)_2H$
TRIEN $NH_2(CH_2CH_2NH)_3H$
TETREN $NH_2(CH_2CH_2NH)_4H$
PENTEN $NH_2(CH_2CH_2NH)_5H$
$\log \beta_n(NH_3) = \log(K_1 \times K_2 \text{ ----- } \times K_n)$
Note that the chelate effect increases with the increase of denticity.

The Ligand Design Rule[10, 11, 12]

The ligand, triquinaldineamine, TQA (Figure-3), which was first synthesized by Karlin,[13] may be a good candidate to act as a sensor for Zn^{2+}. The three quinolyl groups may provide quite good fluorescent properties. It is small and hydrophobic, which may allow it to cross the blood-brain barrier. Third, it may also adopt a tetrahedral structure with Zn^{2+}, which is favored by Zn^{2+}.

The purpose of the research is the synthesis and investigation of the fluorescent sensors, such as TQA[13] for Zn^{2+}, and its applicability to the ligand design concepts developed by Martell and Hancock.[10, 11, 12] This rule is that when one of the chelate rings of a metal-ligand complex increases from a five membered to a six membered ring, the selectivity of the ligand for smaller metal ions, such as Zn^{2+} over larger metal ions such as Cd^{2+} will increase.

Two factors are related to the ligand design rule: the size of the metal ions and the size of the chelate rings. Different sizes of chelate rings favor different sizes of metal ions. Ni^{2+}, Cu^{2+}, Zn^{2+}, Cd^{2+}, Pb^{2+} were selected in this research, because these metal ions' radii ranged in order from small to large, which provides the base to demonstrate binding selectivity of the ligand versus the metal ion radius.

Binding selectivity also depends on the sizes of chelate rings. The five membered rings have different coordination chemistry than the six membered rings. DQPMA and DQPEA were synthesized (Figure-3) and characterized along with TQA. DQPEA may form one six membered chelate ring with metal ions while TQA and DQPMA can form only five-membered rings with metal ions.

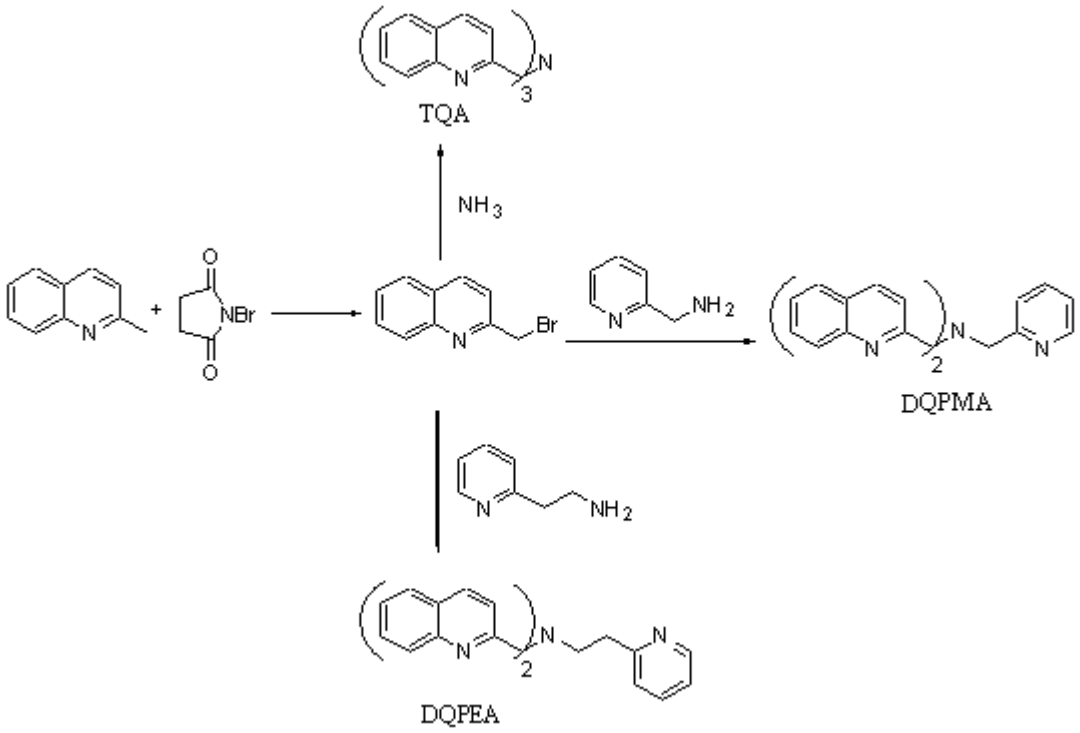

Figure-3. The synthetic scheme for TQA, DQPMA and DQPEA.

In molecules, every atom has a preferred geometry and set of bond lengths to connect to other atoms to form minimum energy compounds. Thus, C prefers to be tetrahedral, which gives C-C-C bond angles of 109.5°, with bond length to other C atoms of 1.54 Å. The deviation from the ideal bond angle or ideal bond length leads to strain energy. Molecules always tend to adopt a minimum energy conformation but usually none of the bond lengths and angles have their ideal values. The strain energy can be mathematically determined by molecular mechanics (MM).[14] MM models geometry modeling strain forces from simple equations. The strain energies of molecules can be calculated, and used to design ligands with higher selectivity for particular ions.

If the MM developed for organic molecules[14] is applied to five membered ring and six membered ring coordinate complexes,[10, 11, 12] it has been determined that the minimum energy metal-ligand complex for six membered chelate rings has a M-N length of 1.6 Å, and N-M-N angle of 109.5° (Figure-4), while has M-N length of 2.5 Å, N-M-N angle of 69.0° for five member ring (Figure-5).[15]

By reference to the low-strain form of cyclohexane,[16] one can understand why change of chelate ring size from five membered to six membered will lead to the lowering of formation constants for large metal ions and increase formation constants for small metal ions.[17] Cyclohexane (Figure-6a) has the lowest steric strain, where all the torsion angles have the ideal value of 60º and the C-C-C bond angles are 109.5º. If one replaces three carbons with two nitrogens and a metal ion in cyclohexane to form a six member ring, one can see that smaller metal ions fit better than do larger metal ions to form lower strain complexes (Figure-6b). The lone pairs on the nitrogen atoms focus best on a metal ion 1.6 Å (Figure-4) away from the nitrogen donors,

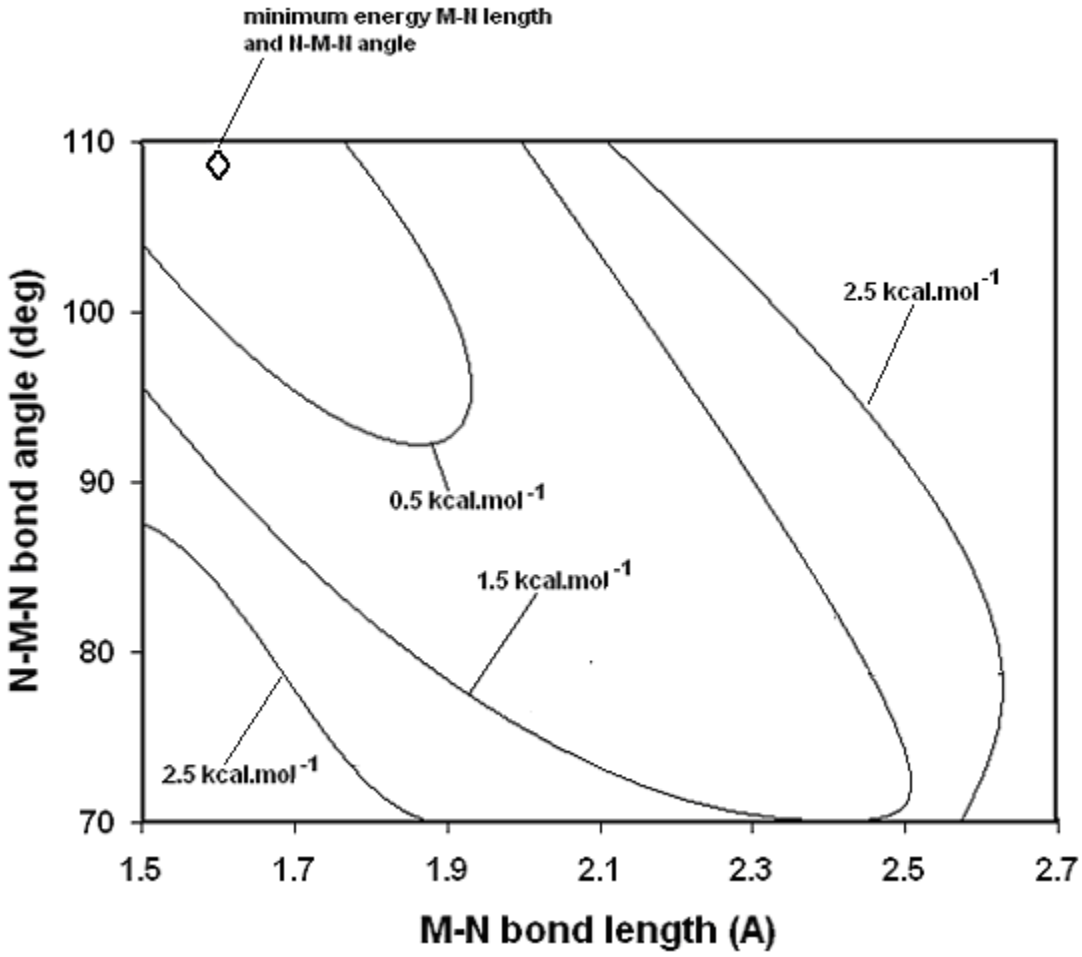

Figure-4. Strain energy of the six membered chelate ring of $NH_2(CH_2CH_2CH_2NH)_3H$ as a function of initial strain free M-N bond length and N-M-N angle.[15]

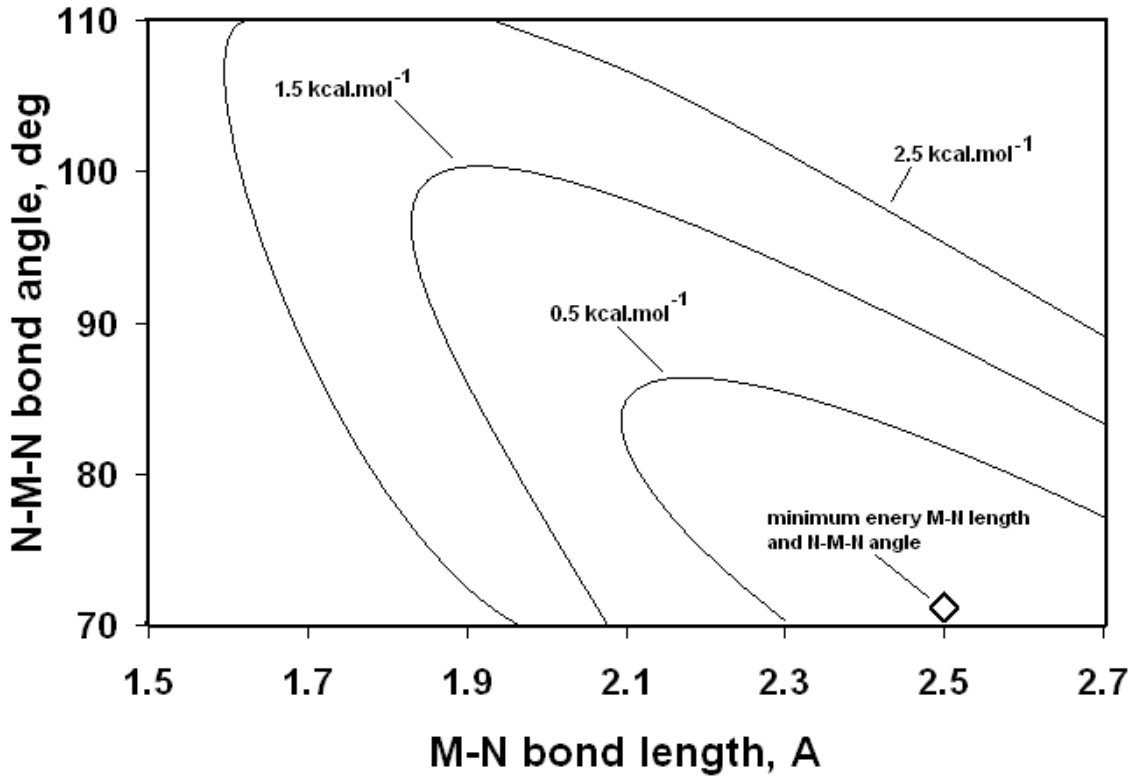

Figure-5. Strain energy of the five membered chelate ring of $NH_2CH_2CH_2NH_2$ as a function of initial strain free M-N bond length and N-M-N angle.[15]

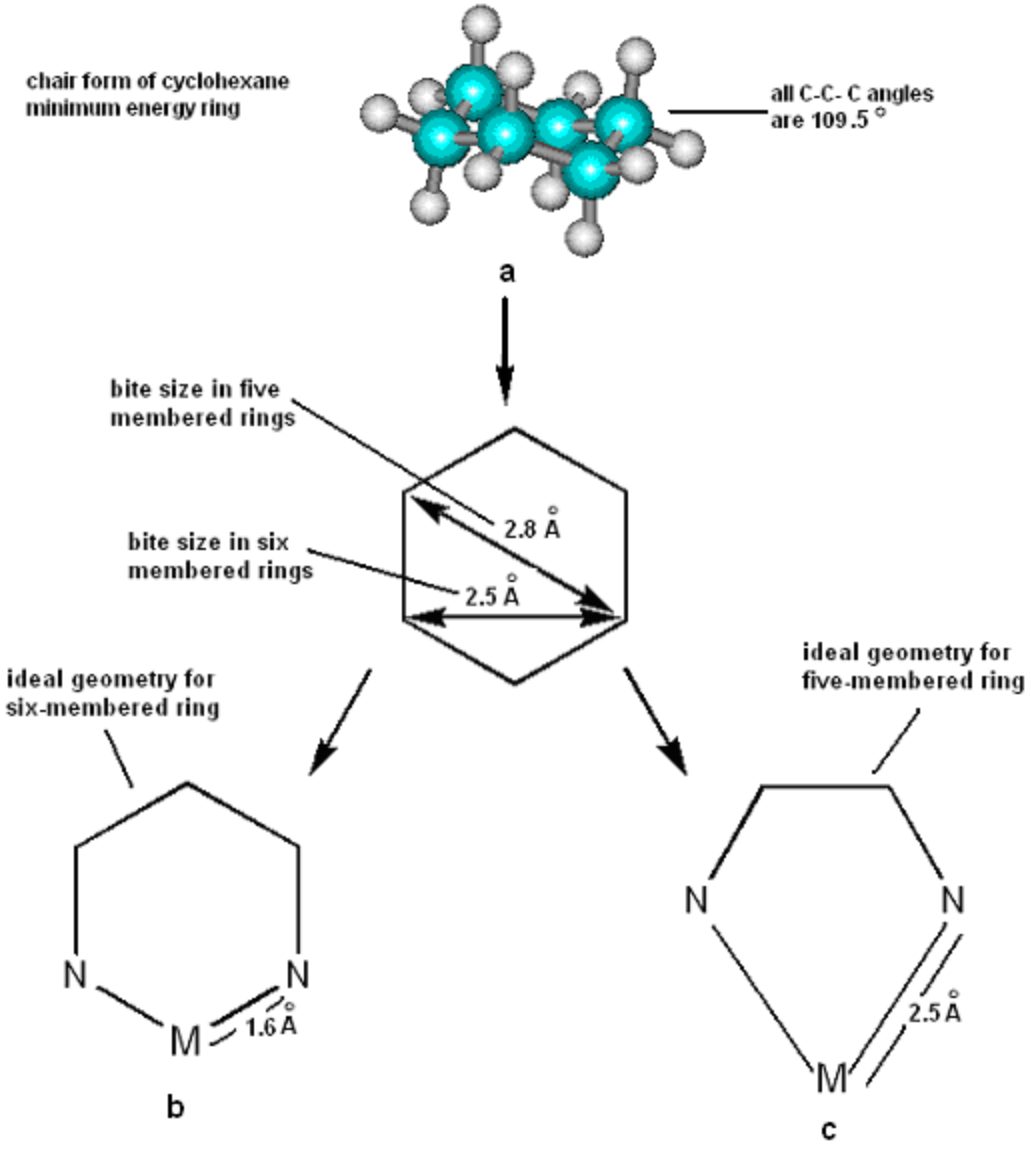

Figure-6. The geometric requirements for a ligand to form minimum strain chelate rings with metals.[17]

which leads to less steric strain for smaller metal ions. If one replaces four carbons with two nitrogens and a metal ion to form a five membered ring, it can be seen that larger metal ions fit better than do smaller metal ions to form lower strain complexes (Figure-6c). The lone pairs on the nitrogens focus best on a metal ion 2.5 Å (Figure-5) away from the nitrogen donors which causes less steric strain for larger metal ions.

Techniques Used in this Study

Potentiometry[18]

The p*Ka* of DQPMA and DQPEA can be determined by collecting data sets of potential (*E*) as a function of the volume of titrant added in sets of acid-base titrations. The standard potential *E*° and a Nernstian slope can be calculated and determined in an acid-base titration. From the potentiometric data above it was possible to calculate values of $\overline{n}$, the number of protons bound per ligand molecule in solution. From such an $\overline{n}$ versus pH curve, it is possible to calculate pK_a's of the ligands.

NMR

NMR is a convenient tool, particularly suited for monitoring proton chemical shifts which change as the environment of the proton changes with different levels of protonation of ligand (L), such as LH^+, LH^{2+}, and so on. The molecular environment influences the absorption of radio-frequency radiation by proton nuclei in a magnetic field, and this effect can be correlated with molecular structure.

Polarography[19]

The study of equilibra by means of polarography has considerable advantages in determining formation constants in solution that are not accessible to other techniques. It can function at concentration levels as low as 10^{-6} *M*, so that it can be applied to the study of poorly soluble ligands such as DQPMA and DQPEA, and to the study of easily hydrolized metal ions.

The essence of the polarographic technique is the production of a polarograhic wave of current as a function of applied potential as electroactive species are reduced at a mercury drop electrode. The polarographic response in the study of complexes of metal ions in solution is of two types. First, if the free ligand, the free metal ion, and metal-ligand complex presenting at the electrode surface reach equilibrium more quickly than the time constant of the polargraphic reduction process, the system is known as a labile system. On the other hand, a non-labile system is defined by the fact that the rate at which equilibrium is reached is slower than that of the polarographic reduction process. For labile systems, one can calculate the formation constant by obtaining the free metal ion concentration through the Lingane equation. But it is the case for non-labile systems.

Fluorescence[2]

Fluorescence techniques are potentially useful in the determination of metal-ligand formation constants, where a low concentration of metal-ligand complex is required. When the concentration of the fluorescent species is low, the fluorescence intensity is proportional to the concentration of that species. Competition experiments can be performed by maintaining the concentration of the ligand constant and changing the ratio of two metal ions. The formation constant ($\log K$) can be calculated by a known formation constant ($\log K_{known}$) plus the substitution constant ($\Delta \log K$) between the two metal ions.

EXPERIMENTAL

General

All solvents were purchased from Burdick & Jackson with the exception of carbon tetrachloride, which was from J.T. Baker. DI water was obtained from the building DI water supply. Tetrachloro-*p*-benzoquinone and 1.0 *N* nitric acid were purchased from Acros. Quinoline, *N*-bromosuccinimide, 2-(2-aminoethyl)pyridine, 2-(2-aminomethyl)pyridine, potassium carbonate, cadmium perchlorate hydrate, zinc perchlorate hexahydrate, nickel(II) perchlorate hexahydrate, copper(II) perchlorate hexahydrate, lead nitrate, sodium perchlorate, sodium nitrate and cadmium nitrate were purchased from Aldrich. Ammonium hydroxide, zinc nitrate and lead nitrate were purchased from Fisher. Silica gel 60 (0.040-0.063 mm, 230-400 mesh) was purchased from EM Science and was used for FCC.[20] Silica gel 60 F_{254} aluminum backed sheets (EM 5574) were used for thin layer chromatography (TLC).

The main physical techniques used in this research were fluorimetry, potentiometry, polarography and NMR spectroscopy.

NMR experiments were performed using a Bruker 400 MHz Avance DRX spectrometer. ^{1}H NMR assignments are given as δ in ppm using $SiMe_4$ as the reference signal (0 ppm) and were verified with ^{1}H-^{1}H COSY. A VWR SR601C pH meter was used for potentiometry experiments; a Metrohm 663 VA stand, a PGSTAT 10 Potentio Stat and GPES program were used for polarography experiments; a FluoroMax-3 was used for fluorescent experiments. A Cary 1E UV-Visible spectrophotometer was used for UV-Vis. Solutions of the ligands were made in methanol and results are given as λ_{max} nm (molar absorbtivity). A Polaris^{TM} FT-IR was used for IR experiments. KBr pellets of the ligands were prepared and selected bands are reported in cm^{-1}. A Buchi R-3000 rotary evaporator and a Welch 1400 Pump were used for concentration.

The protonation constants of DQPMA and DQPEA were determined by collecting data sets of potential (E) as a function of the volume of titrant added in sets of acid-base titrations. The standard potential $E°$ and the Nernst slope was calculated and determined in an acid-base titration.

Synthesis of TQA

Bromoquinaldine. Quinaldine (2.0 mL, 17.0 mmol) and *N*-bromosuccinamide (2.60g, 14.6 mmol) were dissolved in carbon tetrachloride (200 mL) and refluxed for 24 hours under N_2. The resulting mixture was concentrated under reduced pressure and washed with a 50:50 mixture of ether and hexane (3 × 30 mL). After filtration, the organic solution was concentrated under reduced pressure and subjected to FCC[20] using a solvent gradient ranging from 10% to 20% diethyl ether/hexane as the eluant Fractions were analyzed by TLC and those fractions containing the pure product were combined and concentrated to give bromoquinaldine as a light yellow powder (1.51g, 50%); mp 53-54 °C (not found in literature)[13]; ^{1}H NMR ($CDCl_3$) δ 8.19 (d, J = 8.4, 1H), 8.08 (d, J = 8.5, 1H), 7.83 (d, J = 8.1, 1H), 7.72 (td, J_1 = 8.0 .0, J_2 = 1.4, 1H), 7.59-7.27 (m, 2H), 4.72 (s, 2H).

TQA. Bromoquinaldine (2.0 g, 9.6 mmol) was reacted with a 10% excess of 35% ammonium hydroxide solution (223 μL, 3.5 mmol) in tetrahydrofuran (15.0 mL) in the presence of K_2CO_3 (0.62 g, 6.4 mmol) under N_2 at room temperature for 24 hours. The reactant mixture was concentrated by a stream of N_2. Saturated $NaHCO_3$ (10.0 mL) was added and the resulting mixture was extracted with CH_2Cl_2 (3 × 10.0 mL). The combined organic layers were concentrated on a rotary evaporator and subjected to FCC[20] using a mixed solvent of 0.5% triethylamine, 5% methanol, 94.5% dichloromethane. Fractions were analyzed by TLC and those

fractions containing the product were combined, concentrated under reduced pressure and recrystallized from $CHCl_3$/hexane to give TQA (1.27 g, 95%) as a white powder: mp 172-174 °C (not found in literature);[13] ^{1}H NMR ($CDCl_3$) δ 8.14 (d, J = 8.4, 3H), 8.07 (d, J = 8.5, 3H), 7.79 (d, J = 8.1, 3H), 7.75 (d, J = 8.5, 3H), 7.70 (t, J = 7.5, 3H), 7.51 (t, J = 7.2, 3H), 4.14 (s, 6H); UV-Vis (MeOH) 290.0 nm (1.1×10^4), 277.0 nm (8.8×10^3), 243.0 nm (9.0×10^3); IR (KBr) 3058, 2843, 1601, 1506, 1427, 1119, 828, 766 cm^{-1}.

Synthesis of DQPMA

Bromoquinaldine (2.0 g, 9.6 mmol) was reacted with a 10% excess of 2-(2-aminomethyl)pyridine (571 μL, 5.29 mmol) in ethylene dichloride (15 mL) in the presence of K_2CO_3 (0.62 g, 6.4 mmol) under N_2 at room temperature for 24 hours. The reactant mixture was concentrated under reduced pressure. Saturated $NaHCO_3$ (10.0 mL) was added and the resulting mixture was extracted with CH_2Cl_2 (3 × 10.0 mL). The combined organic layers were concentrated on a rotary evaporator and subjected to FCC[20] using a mixed solvent gradient ranging from 5%-10% methanol/dichloromethane. Fractions were analyzed by TLC and those fractions containing the product were combined, concentrated under reduced pressure and recrystallized from $CHCl_3$/hexane to give DQPMA (1.29g, 74%) as a white powder: mp 92-93 °C (not found in literature);[13] ^{1}H NMR ($CDCl_3$) δ 8.54 (d, J = 4.9, 1H), 8.13 (d, J = 8.6, 2H), 8.06 (d, J = 8.6, 2H), 7.79-7.74 (m, 4H), 7.71-7.66 (m, 3H), 7.60 (d, J = 7.9 1H), 7.51(t, J = 7.9, 2H), 4.08 (s, J = 6.2, 2H), 4.08 (s, 4H), 3.97 (s, 2H); UV-Vis (MeOH) 290.0 nm (7.2×10^3), 277.0 nm (5.8×10^3), 243.0 nm (8.6×10^3); IR (KBr) 3058, 2819, 1600, 1590, 1506, 1425, 827, 755 cm^{-1}.

Synthesis of DQPEA

Bromoquinaldine (2.0 g, 9.62 mmol) was reacted with a 10% excess of 2-(2-aminoethyl)pyridine (632 μL, 5.29 mmol) in ethylene dichloride (15 mL) in the presence of K_2CO_3 (0.62 g, 6.4 mmol) under N_2 at room temperature for 24 hours. The reactant mixture was concentrated under reduced pressure. Saturated $NaHCO_3$ (10.0 mL) was added and the resulting mixture was extracted with CH_2Cl_2 (3 × 10 mL). The combined organic layers were concentrated on a rotary evaporator and subjected to FCC[20] using a mixed solvent gradient ranging from 5%-10% methanol/dichloromethane. Fractions were analyzed by TLC and those fractions containing the product were combined, concentrated under reduced pressure and recrystallized from $CHCl_3$/hexane to give DQPEA (1.41 g, 76%) as a white powder: mp 116-117 °C (compound not found in literature); ^{1}H NMR ($CDCl_3$) δ 8.44 (d, J = 0.9, 1H), 8.06-8.03 (m, 4H), 7.77 (dd, J_1 = 8.0, J_2 = 1.2, 2H), 7.68 (td, J_1 = 7.0 J_2 = 1.4, 2H), 7.54 (d, J = 8.5, 2H), 7.51-7.48 (m, 3H), 7.09 (tt, J_1 = 5.4, J_2 = 1.0, 1H), 7.05 (d, J = 7.8, 1H), 4.09(s, 4H), 3.10-3.10-3.08 (m, 4H); UV-Vis (MeOH) 290.0 (1.1×10^4), 277.0 (9.0×10^3), 243.0 (1.3×10^4); IR (KBr) 3062, 2835, 1599, 1506, 1427, 828 cm^{-1}.

X-Ray Crystallographic Study of Zn^{2+}-DQPEA and Cd^{2+}-DQPEA

DQPEA (0.050 g, 0.12 mmol) and zinc perchlorate hexahydrate (0.045 g, 0.12 mmol) or cadminum nitrate (0.041 g, 0.12 mmol) in 20 ml were dissolved in 20 ml 95% ethanol in a 50 ml beaker. The beaker was sealed with parafilm with several small holes on the film. Crystals appeared 3-4 weeks later after half of the solvent evaporated. Crystals were sent to the Chemistry

Department at Texas A&M University for crystal structure analysis. HyperChem Std. 5.1 drawings were used for graphical representation of the X-ray data.

The CHEF Effect in TQA Complexes with Zn^{2+}, Cd^{2+}, Pb^{2+}, Cu^{2+}, Ni^{2+}

Solutions (1.0×10^{5} *M*) were prepared of Zn^{2+}-TQA, Cd^{2+}-TQA, Pb^{2+}-TQA, Cu^{2+}-TQA, Ni^{2+}-TQA by dissolving TQA with $Cd(ClO_4)_2$, $Zn(ClO_4)_2$, $Ni(ClO_4)_2$, $Cu(ClO_4)_2$, or $Pd(NO_3)_2$ in 1:1 ratio in 50% methanol/water solvent. A VWR SR601C pH meter was used to test the pH of all the solutions, which were around 6.7. Fluorescence intensity was recorded at the excitation wavelength of 310 nm and emission wavelength of 450 nm. (Appendix-1)

Calibration of the Glass Electrode

Acid - base titrations were carried out daily for calibration of the glass electrode system used. A primary standard 1.000 *N* HNO_3 was used to prepare a 0.010 *M* HNO_3 secondary standard solution. The ionic strength of the solutions was kept constant at $I = 0.10$ with $NaNO_3$. A base solution with the concentration of about 0.010 *M* NaOH was also prepared, and standardized with the acid secondary standard solution. 25 mL of the acid solution was placed in a temp. controlled cell, which was thermostatted to 25.00 ± 0.05 °C. Nitrogen was bubbled through the solution during titrations to exclude CO_2. The acid was titrated with 50 mL base with 1mL increments. The potentials were recorded on a VWR SR601C pH meter, reading to ±0.1 mV. The titration was used to standardize the 0.01 *M* NaOH from the midpoint of the curve of mV versus volume of base added (Figure-7a). From the known concentrations of the acid and base, the pH was calculated for each titration point. The standard potential $E°$ and the Nernst slopes were determined by drawing pH versus potential plot (Figure-7b) in this titration

Determination of Protonation Constants for DQPMA and DQPEA

The protonation constants of DQPMA and DQPEA were determined by collecting data sets of potential (E) as a function of the volume of titrant added in sets of acid-base titrations.

K_{a1} for DQPMA was determined by titrating 50 ml of 10^{-4} M DQPMA, 0.1 M $NaNO_3$ solution with secondary standard 4.0×10^{-4} M HNO_3 in the above temp. controlled cell. The ionic strength of the solutions was kept constant at $I = 0.10$ with $NaNO_3$. From the potentiometric data obtained it was possible to calculate values of $\bar{n}$, the number of protons bound per ligand molecule in solution. From such an $\bar{n}$ versus pH curve, it was possible to calculate the first pK_a of the ligand, as well as the second. The theoretical $\bar{n}$ versus pH curve can be calculated from the mass balance equation for the proton:

$$[H_T] = [H^+] + [LH^+] + 2[LH_2^{2+}] \qquad [1]$$

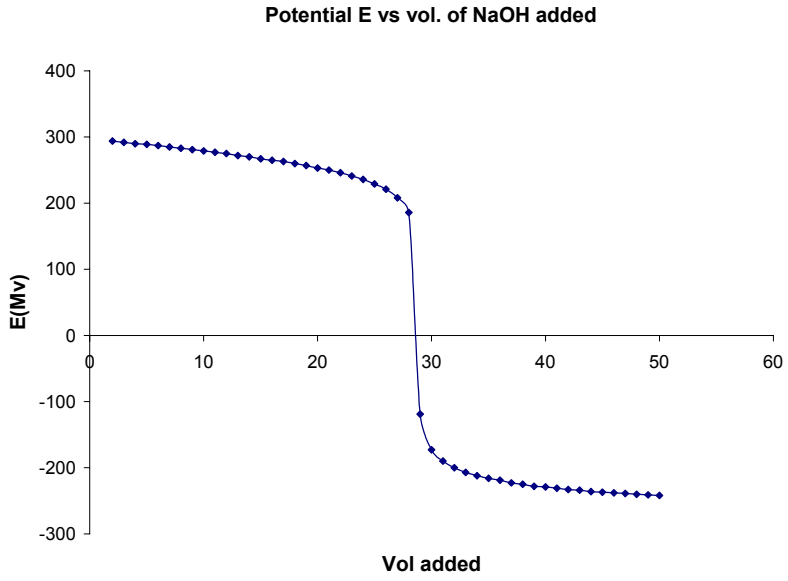

a

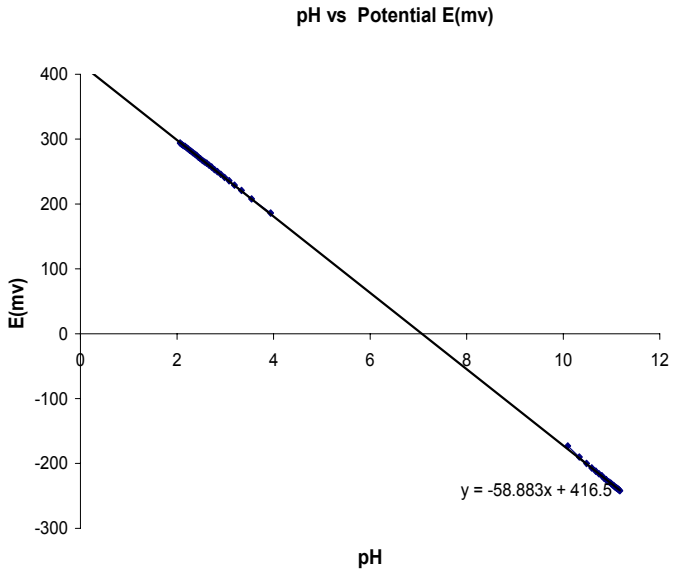

b

Figure-7. The acid-base titration for calibration of the glass electrode.

where L is the ligand, H_T is the total concentration of proton in solution, and LH^+ and LH_2^{2+} are the monoprotonated and diprotonated forms of the ligand. The first and second protonation constants, K_{a1} and K_{a2}, are given by:

$$K_{a1} = [HL^+]/[H^+][L] \qquad [2]$$

$$K_{a2} = [H_2L^{2+}]/[H^+][LH^+] \qquad [3]$$

Rearranging the protonation constants and inserting them into the mass balance equation we obtain:

$$[H_T] = [H^+] + K_{a1}[L][H^+] + 2K_{a1}\bullet K_{a2}[L][H^+]^2 \qquad [4]$$

from which is obtained:

$$[H_T] - [H^+] = [L]\{K_{a1}[H^+] + 2K_{a1}\bullet K_{a2}[H^+]^2\} \qquad [5]$$

Since $\bar{n}$ is defined as the ratio of total concentration of protons bound to the ligand to total ligand concentration, we have

$$\bar{n} = ([H_T] - [H^+])/[L_T] \quad [6]$$

we can use the expression for the mass balance equation for the ligand to calculate $[L_T]$:

$$[L_T] = [L] + [LH^+] + [LH_2^{2+}] \quad [7]$$

which on insertion of the expressions for K_{a1} and K_{a2} (eq. 2 and 3) becomes:

$$[L_T] = [L] + K_{a1}[L][H^+] + K_{a1}\bullet K_{a2}[L][H^+]^2 \quad [8]$$

from which we obtain by replacing [LT] in equation [6] with equation [8]:

$$\bar{n} = (K_{a1}[H^+] + 2K_{a1}\bullet K_{a2}[H^+]^2)/(1 + (K_{a1}[H^+] + K_{a1}\bullet K_{a2}[H^+]^2\} \quad [9]$$

The solubility of DQPEA (5.0×10^{-5} *M*) is considerably lower than that for DQPMA (10^{-4} *M*), which meant that lower concentrations of the ligand had to be used. K_{a1} for DQPEA was determined by titrating 5.0×10^{-5} *M* DQPEA solution with secondary standard 2×10^{-4} *M* HNO_3 solution. The titration was carried out at 25.0ºC $\pm$0.5ºC, and purified N_2 gas was bubbled through the solution to exclude CO_2.

K_{a2} and K_{a3} were determined by titrating 1.0×10^{-3} *M* DQPMA or 1.0×10^{-3} *M* DQPEA dissolved in 5.0×10^{-3} *M* HNO_3 solution with 5.0×10^{-3} *M* NaOH.

All titrations were carried out at 25.0ºC $\pm$0.5ºC and saturated with prepurified N_2 gas. The ionic strength of the solutions was kept constant at $I = 0.10$ with $NaNO_3$. And all NaOH solution were standardized by a previously standardized dilute solution of HNO_3.

Determination of K_{a2} for DQPMA by NMR

The accuracy of K_{a2} determined by glass electrode potentiometry, was considered to be possibly less accurate than desired because of the low concentration of the ligand, and its surpisingly low value compared to other similar ligands. It was therefore decided to check the value of K_{a2} by a ^{1}H NMR experiment. A series of solutions with 0.1% Sodium-2, 2-dimethyl-2-silapentane -5-sulfonate, 10% D_2O, 0.1 *M* $NaNO_3$, 0.01 *M* DQPMA at different pH values were prepared. pH values for these solutions were adjusted from 1 to 4.5 with increments of about 0.3 pH units. All proton signals were assigned based on a ^{1}H^{1}H·COSY experiment. The signal for H_{q4} (shown in Appendix-#) on the pyridine group of DQPMA was elected as reference to measure the ^{1}H NMR shift as a function of pH. A pH versus H_{q4} shift plot was drawn from the data obtained above. The pK_a is indicated by midpoints in the regions of shifting of the ^{1}H signal as a function of pH.

Determination of the Formation Constant (K_1) of DQPMA and DQPEA with Cd^{2+} by Polarography

A $Cd(NO_3)_2$ (50.0 mL, 5.0×10^{-5} *M*) solution was placed in the titration cell of the polarograph (Metrohm 663 VA stand and Autolab electronic control system) , which was thermostatted to 25.0 ±0.5 °C. The pH of the solution was monitored using a VWR SR601C pH meter. This was titrated with DQPMA (1.0×10^{-4} *M*) or DQPEA (5.0×10^{-5} *M*). The ionic strength of the solutions was kept constant at I = 0.10 with $NaNO_3$. Differential pulse voltammetry measurements were carried out using a Model 663 VA Stand (Metrohm) polarograph. Before titration, the $Cd(NO_3)_2$ solution was allowed to equilibrate and degas for 10 minutes in the absence of the mercury electrode. Peaks were recorded in the differential pulse (DP) mode of the instrument and a modulation amplitude of -0.02505 V per second over the potential range of -0.2 to -1.0 was set. When excess of the ligands appeared (after equivalence point), the system was in

labile condition and a set of potential *E* data was collected responding to addition of l mL ligands.

Determination of Formation Constant of DQPMA and DQPEA with Zn^{2+}, Ni^{2+}, Cu^{2+}, Pb^{2+} by Fluorimetry

The competition experiments were carried out for the calculation of the formation constants of the complexes of the ligands with Zn^{2+}, Ni^{2+}, Cu^{2+}, Pb^{2+}. The data were recorded at the excitation wavelength of 265 nm and emission wavelength of 375 nm, 0.1 second time integration and 2 averaged scans were set over all the experiments. Sets of fluorescent date were collected separately responding to different Cd^{2+}: ligand : Zn^{2+} ratios for Zn^{2+}, Zn^{2+}:ligand:Cu^{2+} ratios for Cu^{2+}, Zn^{2+} : ligand : Ni^{2+} ratios for Ni^{2+}, Zn^{2+} : ligand : Pb^{2+} ratios for Pb^{2+}. The concentration of ligands was kept constant at $1.0\times 10^{-4}M$. The concentration of metal ions are given in tables 5-9.

Determining the pH range of CHEF Effect for Zn^{2+}-DQPEA Complex

A solution of Zn^{2+}-DQPEA (5.0×10^{-5} *M*) complex was prepared by dissolving $Zn(ClO_4)_2$ and DQPEA in 1:1 ratio in DI water. The pH of solution was adjusted from 2.0 to 13.0 by adding HNO_3 and NaOH. Fluorescence measurements were taken at each pH value. The excitation wavelength was 265 nm; the emission wavelength was 374 nm.

Determining the Fluorescence Intensity as A Function of The Concentration of Zn^{2+}-DQPEA

The Zn^{2+}-DQPEA (1.0×10^{-5} *M*) complex was prepared by dissolving $Zn(ClO_4)_2$ and DQPEA in 1:1 ratio in DI water. The solution was diluted by adding DI water to 8.0×10^{-6} *M*, 6.0

$\times 10^{-6}$ *M* , 4.0×10^{-6} *M*, 2.0×10^{-6} *M*, 10^{-6} *M* , 5.0×10^{-7} *M* . Fluorescence intensities were measured for each concentration. The excitation wavelength was 265 nm; the emission wavelength was 374 nm.

RESULTS AND DISCUSSION

Characterization of TQA, DQPMA and DQPEA

It is shown in the ^{1}H NMR spectrum of TQA (Appendix-1) that aromatic peaks between 7.4 to 8.2 ppm integrate for a total of 6H. A singlet at 4.1 ppm, which integrates for 2H, is present and assigned as the methylene signal of TQA.[21] This is consistent with the molecular structure of TQA where there are three quinaldine groups are bonded to a nitrogen, so every one-proton aromatic peak represents 3 protons from each of the 3 quinaldine groups, and the two-proton methylene peak (δ = 4.14 ppm) represents the 3 methylene groups.

TQA has no CHEF effect with Pb^{+2}, Ni^{+2}, Cu^{+2}, while it does have a CHEF effect with Zn^{2+} and Cd^{+2} (Figure-8, Appendix-2). The Zn^{2+}-TQA complex is ten times stronger, in terms of fluorescence intensity, than the Cd^{2+}-TQA complex (Figure-8). The unpaired electrons on Ni^{+2} and Cu^{+2} and the lone pair electrons on Pb^{+2} may contribute the quenching of the fluorescence for these complexes.[2]

Based on the CHEF effect of TQA with Zn^{2+}, Cd^{2+}, Ni^{2+}, Cu^{2+}, Pb^{2+} and the insolubility of TQA in water, DQPMA and DQPEA were synthesized to improve the solubility of the complex in water and to investigate the ligands' selectivity for smaller vursus larger metal ions.

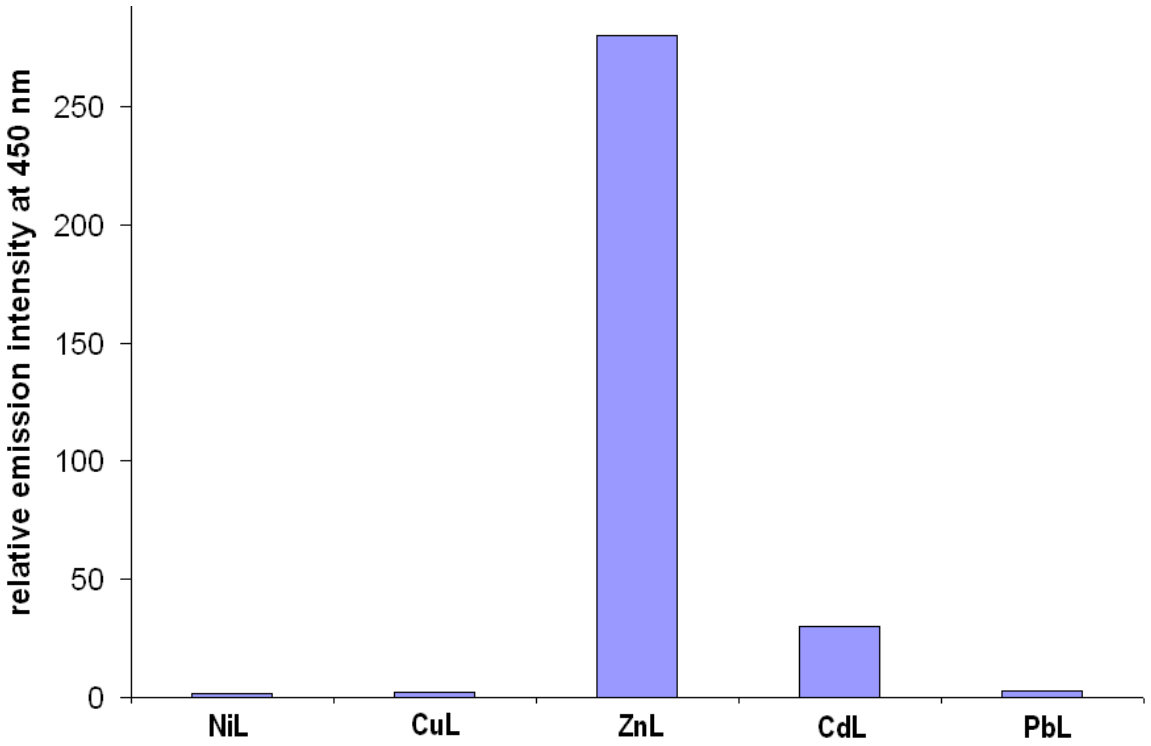

Figure-8. Relative emission intensity of metal complexes with TQA (1.0×10^{-5} *M*) at 450 nm.

Identification of DQPMA was based on the ^{1}H NMR spectrum (Appendix-3), the ^{1}H-^{1}H·COSY spectrum (Figure-9) and on literature chemical shifts of pyridine and quinaldine protons.[21] The peaks at 4.0 ppm and 4.1 ppm integrate as 2H and 4H, and represent the methylene protons of methyl pyridine and the methylene protons of the two quinaldines respectively. In the aromatic region individual protons of pyridine ring integrate as 1H while individual protons of the two quinaldine rings integrate as 2H.[21] (Appendix-3)

Identification of DQPEA was based on ^{1}H NMR spectrum (Appendix-4) and ^{1}H-^{1}H·COSY NMR spectrum (Figure-10) and on literature chemical shifts of pyridine and quinaldine protons.[21] The peaks at 3.3 ppm and 4.2 ppm both integrate as 4H, and represent the ethylene protons of ethyl pyridine and the methyllene protons of the 2 quinaldines. In the aromatic region individual protons of pyridine ring integrate as 1H while individual protons of the 2 quinaldine rings integrate as 2H.[21] (Appendix-4)

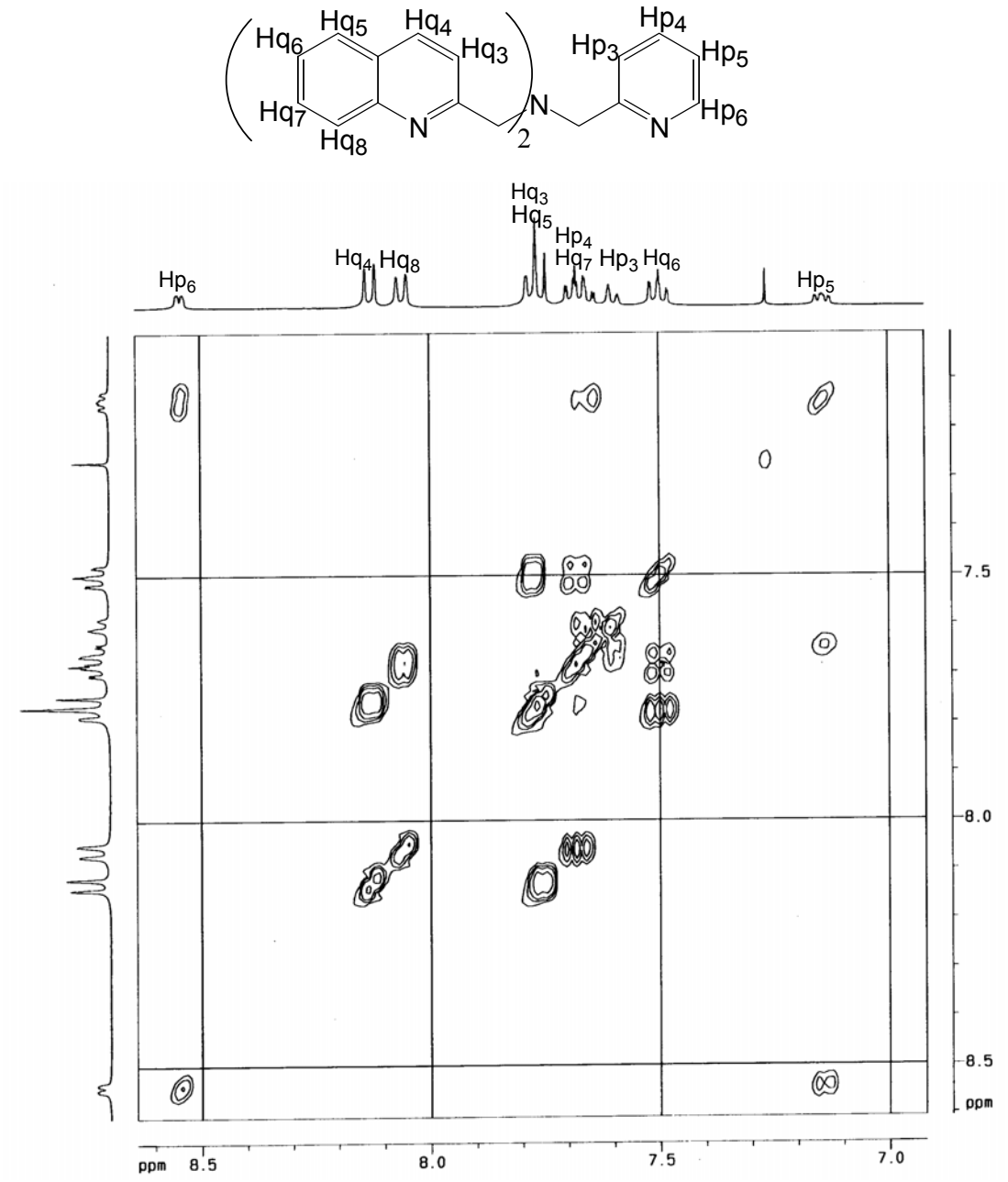

Figure-9. $^{1}H^{1}H$·COSY NMR spectrum of DQPMA.

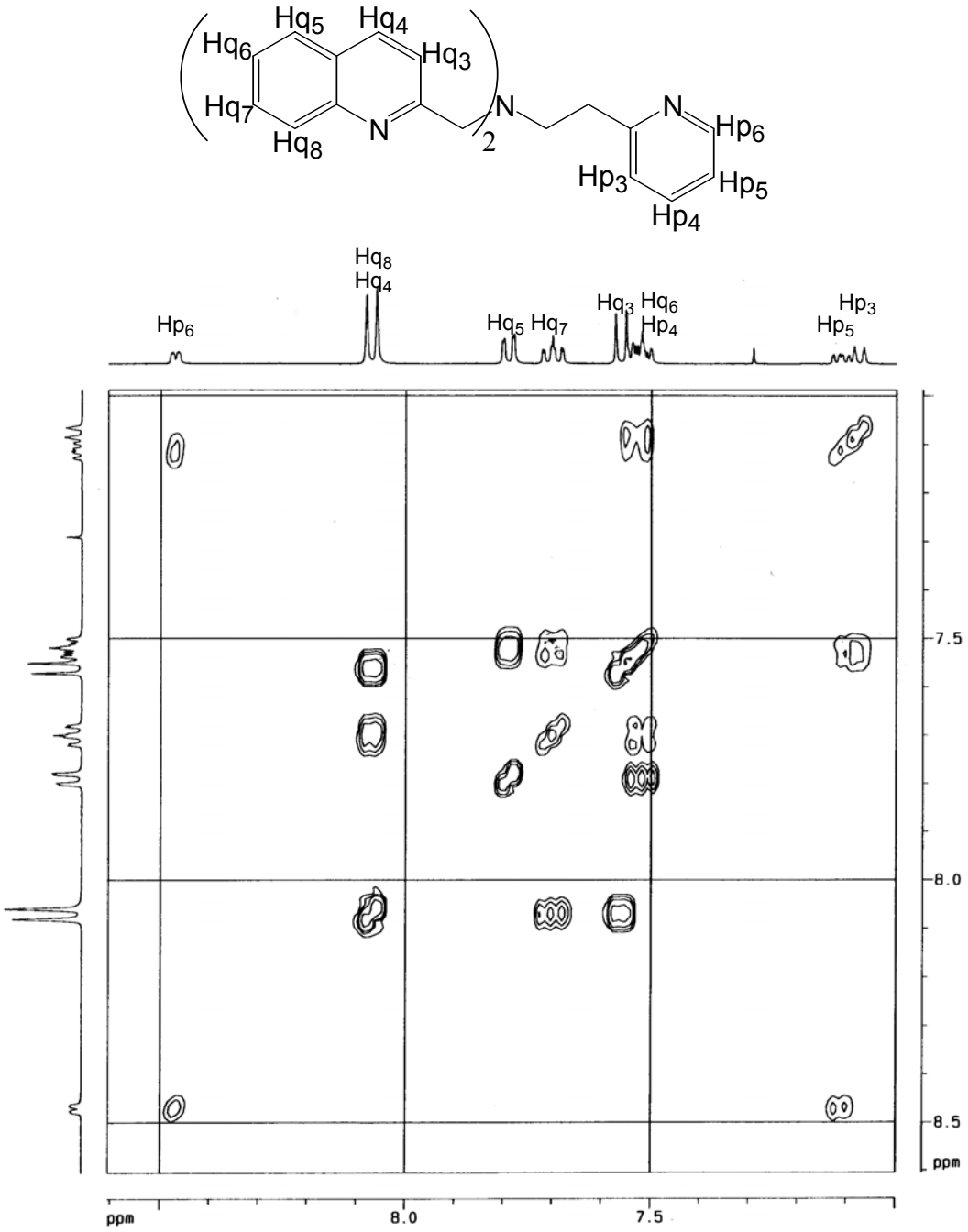

Figure-10. $^{1}H^{1}H$·COSY NMR spectrum of DQPEA

The Crystal Structure of Zn^{2+}-DQPEA and Cd^{2+}-DQPEA

Hyperchem (Std. 5.1) drawings of the crystal structures of Zn^{2+}-DQPEA and Cd^{2+}-DQPEA are shown in Figures 11 and 12. ORTEP figures and data tables are provided in Appendices 5-12.

The angle N(1)-Zn^{2+}(1)-N(4) in the six-membered ring of Zn^{2+}-DQPEA is 103.36° while the N(1)-Cd^{2+}(1)-N(4) angle in the six-membered ring of Cd^{2+}-DQPEA is 91.56°, which indicates that the six-membered ring of Zn^{2+}-DQPEA is closer to the predicted ideal N-Metal-N angle of 109.5° than Cd^{2+}-DQPEA (Figure-6).[17] This may result in an increase in the selectivity of the ligand for Zn^{2+} over Cd^{2+} when DQPMA is replaced by DQPEA.

The X-ray structure also shows that Cd^{2+} is six coordinated while Zn^{2+} is five coordinated. The Cd^{2+} ion is larger than Zn^{2+}, which may provides more room for coordination.

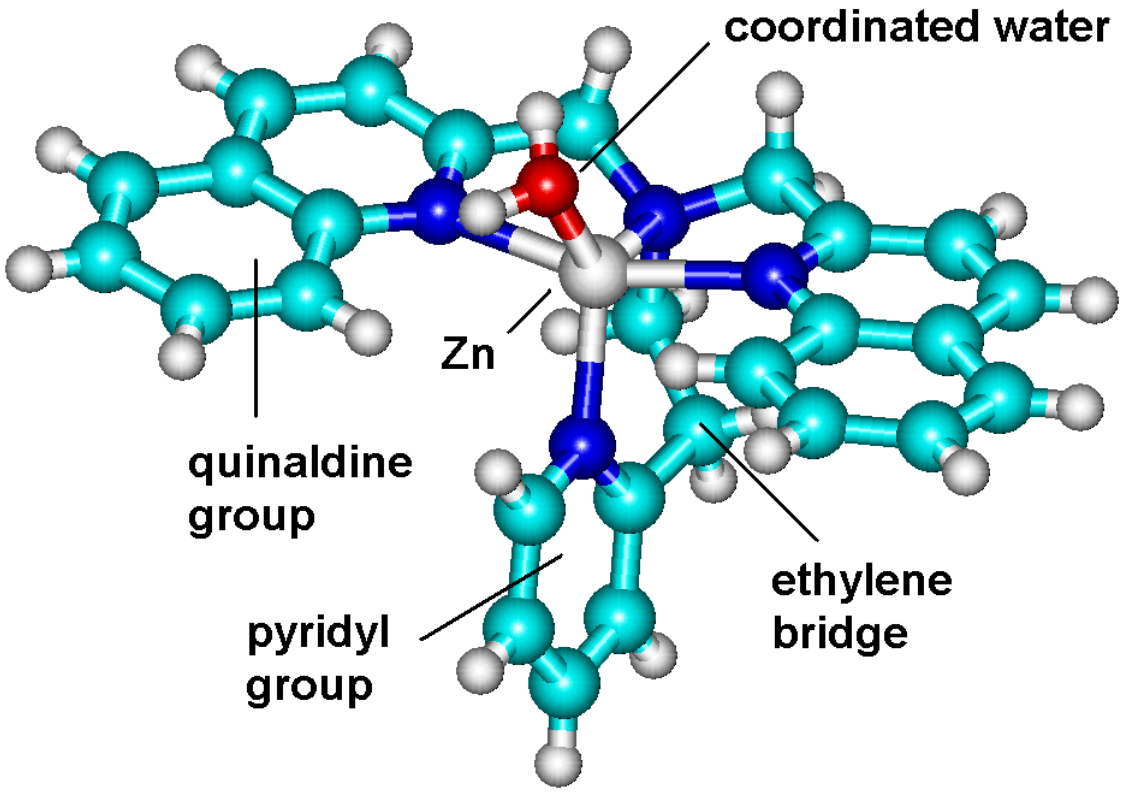

Figure-11. HyperChem (Std. 5.1) drawing of the crystal structure of Zn^{2+}-DQPEA (also see Appendices 5-8)

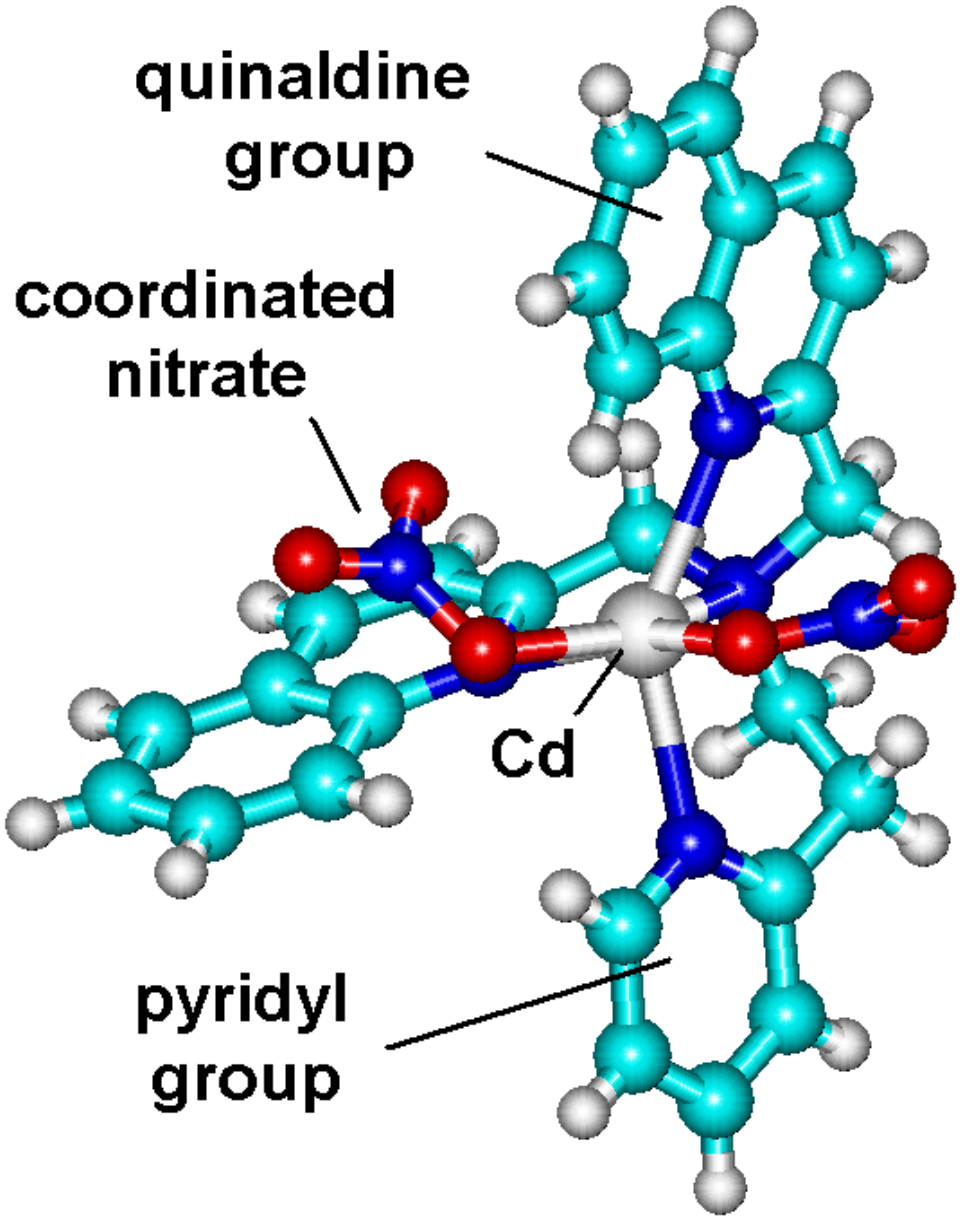

Figure-12. HyperChem (Std. 5.1) drawing of the crystal structure of Cd^{2+}-DQPEA (also see Appendices 9-12).

The pK_a values of DQPMA and DQPEA

In a calibration acid-base titration, the Nernst slope should be close to the theoretical value of 59.16 mV per decade, i.e. per pH unit, for a one-electron process. In the example (Figure-7b) the slope is 58.88 mV/decade, very close to the theoretical value. Acceptable ranges for Nernst slope were from 58 to 61mV per decade, with the standard potential $E°$ at 412 mv to 420 mv. The variation is thought to arise because of the changes of surface structure of the glass with time. This is why it is necessary to calibrate the pH meter daily before each use.

Determination of pK_{a1}

Once the pH meter has been calibrated, it is ready for use to determine the pK_a of the ligands. Because the solubility of DQPMA and DQPEA is low, pK_a values of the two ligands are determined in two steps. K_{a1} for DQPMA was determined by titration of 25 mL 1.0×10^{-4} *M* DQPMA with 50 mL 4.0×10^{-4} *M* HNO_3. K_{a1} for DQPEA was determined by titration of 25 mL 5.0×10^{-5} *M* DQPMA with 50 mL 2.0×10^{-4} *M* HNO_3. K_{a2} and K_{a3} were measured by titration of 25 ml of 1.0×10^{-3} *M* DQPMA or DQPEA in 5.0×10^{-3} *M* HNO_3 with 50 ml 5.0×10^{-3} *M* NaOH.

The method for calculation of K_{a1} is as follows:

For an aqueous solution of the ligands, the total concentration of the ligand L_{total} and the total concentration of H^+_{total} are given by the equations:

$$L_{total} = L_{free} + HL^+ + H_2L^{2+} + H_3L^{3+} \quad (1)$$

$$H^+_{total} = H^+_{free} + H^+_B = H^+_{free} + HL^+ + 2H_2L^{2+} + 3H_3L^{3+} \quad (2)$$

A set of data for potentials (E) versus volume of HNO_3 was collected from the titration of the ligand with HNO_3. With this data and the calibrated Nernst slope and $E°$ obtained from the

acid versus base titration (Figure-7b), A set of the $\bar{n}$ versus pH curves could be calculated by applying the fallowing equations:

$$pH = (E° - E)/slope \quad (3)$$

$$H^{+}_{free} = 10^{-(E° - E)/slope} \quad (4)$$

$$H^{+}_{B} = (vol.acid \times conc.acid/total.vol) - H^{+}_{free} \quad (5)$$

$$\bar{n} = H^{+}_{B} / L_{total} \quad (6)$$

The plots of $\bar{n}$ versus pH were drawn from the calculation above (Figure-13 and Figure-14).

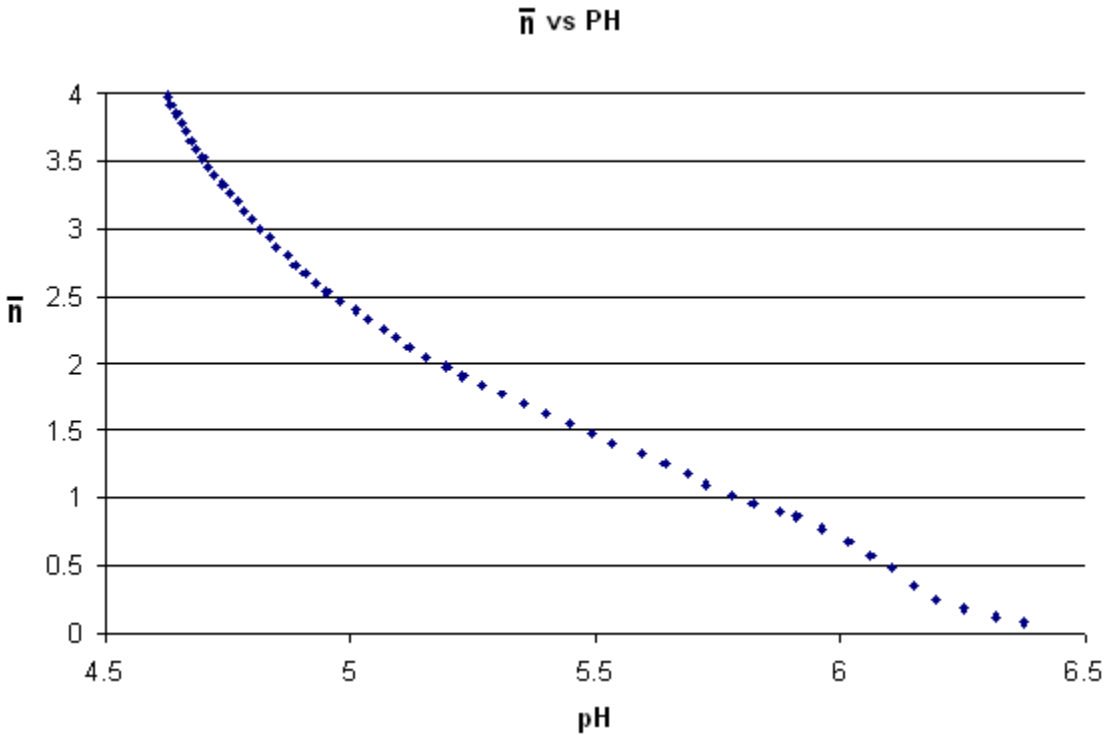

Figure-13. $\bar{n}$ versus pH for DQPMA (1.0×10^{-4} *M*) to determine pK_{a1}= 6.15.

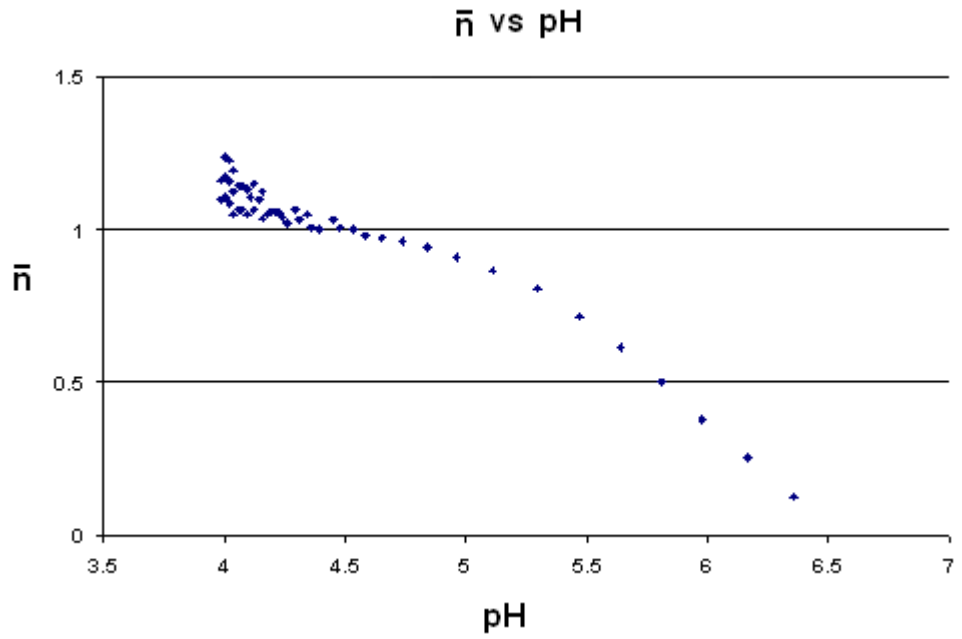

Figure-14. $\bar{n}$ versus pH for DQPEA (5.0×10^{-5} *M*) to determine pK_{a1}= 5.75.

When the pH region of the first protonation point was reached, the dominant equilibrium was:

$$LH^+ = L + H^+$$

then $LH^+ > H_2L^{2+} + H_3L^{3+}$

and $H^+_B = HL^+$ and $L_{total} = L_{free} + HL^+$

When $\bar{n} = H^+_B / L_{total} = 1/2$

then $HL^+ = L_{free} = 1/2\ L_{total}$

and $pK_{a1} = -\log ((L_{free} \times H^+_{free})/HL^+) = -\log H^+_{free} = pH$

pH values of 6.12 for DQPMA and pH = 5.75 for DQPEA were observed for values of $\bar{n}$ was 0.5, so that pK_{a1} for DQPMA is 6.12 and pK_{a1} for DQPEA is 5.75. These are comparable with tri-2-pycolylamine (TPA), whose pK_{a1} is 6.10.[22] However the whole curve is does not closely follow the theoretical curve,[18] possibly due to the low concentration (1.0×10^{-4} *M* for DQPMA and 5.0×10^{-5} M for DQPEA). At this level a small error in concentration of acid will lead to a considerable error in calculated values of $\bar{n}$. Therefore, the pK_{a2} and pK_{a3} needed to be determined by a different method.

Determination of pK_{a2} and pK_{a3}

A glass electrode potentiometric titration was carried out to obtain a set of potential versus added volume of NaOH by titration of 25 ml of 10^{-3} *M* ligand in 5.0×10^{-3} *M* HNO_3 solution with 5.0×10^{-3} *M* NaOH. With this data plus the Nerst slope and *E*° obtained from acid versus base titration, a plot of $\bar{n}$ versus pH could be calculated by applying equations (3), (4), (6) as well as the following :

$$H^+_B = (\text{vol.acid} \times \text{conc.acid} / \text{tot.vol.}) - H^+_{free} - (\text{vol.base} \times \text{conc.base}/\text{tot.vol.}) \quad (7)$$

Thus, the plots of $\bar{n}$ versus pH were drawn based on the calculation above (Figure-15-16).

When the pH region where the second protonation constant is dominant:

$$H_2L = HL + H^+$$

$$[H_2L] >> [H_3L] + [L]$$

So that $H^+_B = 2H_2L + HL$ and $L_{total} = HL + H_2L$

If $\bar{n} = H^+_B / L_{total} = 1.5$

Then $HL = H_2L = 1/2\ L_{total}$

So $pK_{a2} = -\log((HL \times H^+_{free})/H_2L) = -\log H^+_{free} = pH$

When the pH region where the third protonation constant is dominant is reached:

$$H_3L = H_2L + H^+$$

$$H_3L >> HL + L$$

So $H^+_B = 2H_2L + 3H_3L$ and $L_{total} = H_2L + H_3L$

If $\bar{n} = H^+_B / L_{total} = 2.5$

Then $H_3L = H_2L = 1/2\ L_{total}$

So $pKa_3 = -\log((H_2L \times H^+_{free})/H_3L) = -\log H^+_{free} = pH$

The pK_{a2} for DQPMA was determined to 3.20 (Figure-15). From this graph, pK_{a3} can not be determined at the concentration of the 10^{-3} *M* level. For DQPMA pK_{a2} = 4.30 and pK_{a3} = 2.90.

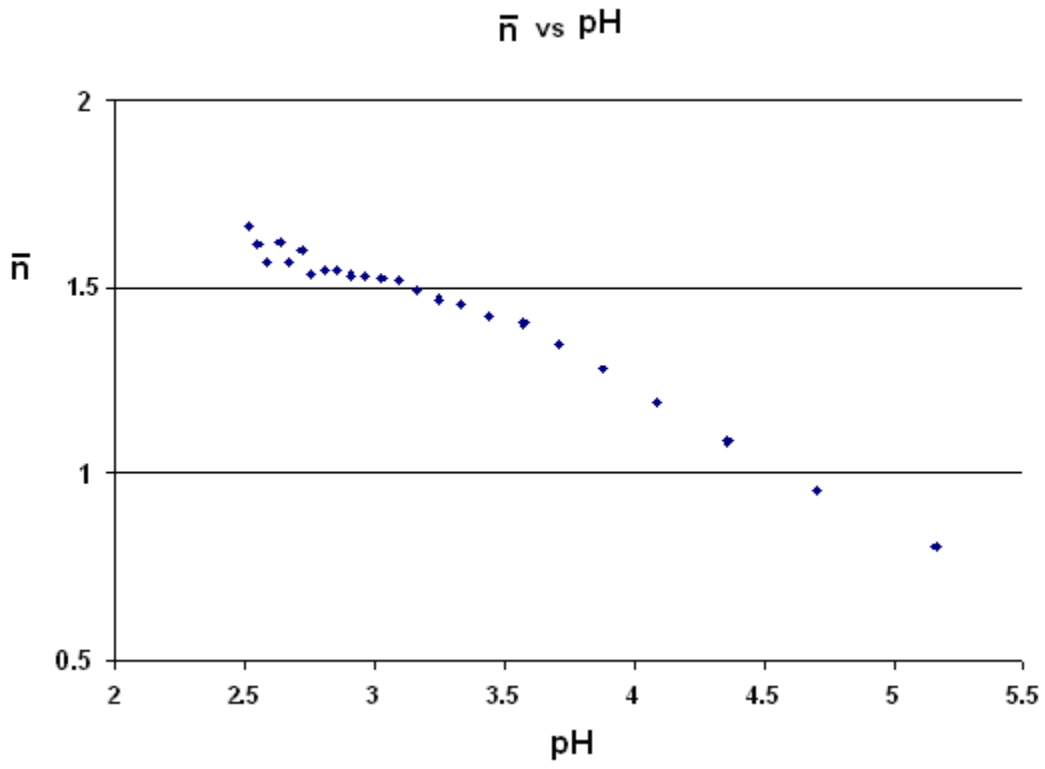

Figure-15. $\bar{n}$ versus pH for DQPMA (1.0×10^{-3} *M*) used to determine pK_{a2} = 3.2.

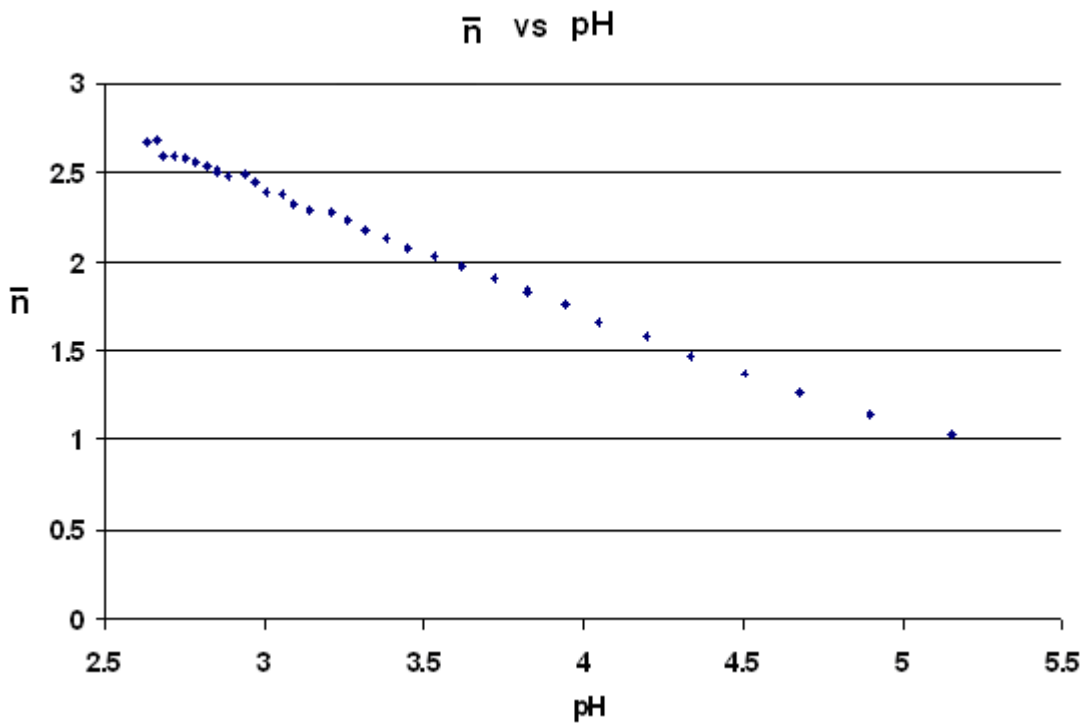

Figure-16. $\bar{n}$ versus pH for DQPEA (1.0×10^{-3} *M*) used to determine pK_{a2} = 4.31 and pK_{a3} = 2.90.

pK_{a2} for DQPMA by NMR

The pK_a's for DQPMA, DQPEA TPA are listed in Table-2. The pK_a's for DQPEA (pK_{a1} = 5.75, pK_{a2} = 4.31, pK_{a3} = 2.90) are similar to the pK_a's of TPA (pK_{a1} = 6.10, pK_{a2} = 4.28, pK_{a3} = 2.49).[22] Only two pK_a's could be determined for DQPMA. Therefore, in order to check the accuracy of the value determined for pK_{a2} for DQPMA, a series of ^{1}H NMR experiments were carried out with DQPMA (Figure-17). The proton which showed the largest chemical shift as a function of pH was the proton H_{q4}, compared to the other quinaldine and pyridine protons (Figure-9). From the plot of the chemical shift of the H_{q4} versus pH (Figure-18). It can be concluded that pK_{a2} is around 2.8, which is very close to 3.15 as determined by potentiometry.

The reason for the differences in pK_a's between DQPMA versus DQPEA probably arises because the DQPEA has one more methylene group than DQPMA does.

Table-2. pK_a for DQPMA and DQPEA (from potentiometry)

	p*Ka* for DQPMA	p*Ka* for DQPEA	p*Ka* for TPA[22]
$LH^+ = L + H^+$	6.15	5.75	6.10
$LH^+_2 = LH^+ + H^+$	3.15	4.31	4.28
$LH^+_3 = LH^+_2 + H^+$		2.90	2.49

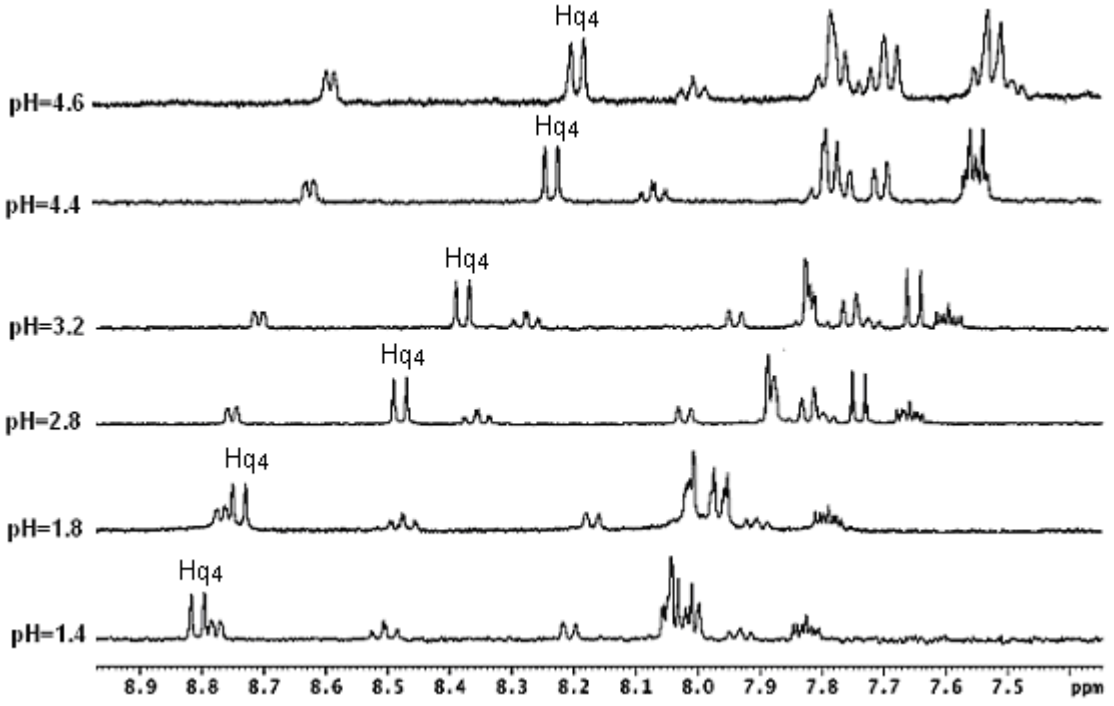

Figure-17. ^{1}H NMR of DQPMA (1.0×10^{-3} *M*) as a function of pH.

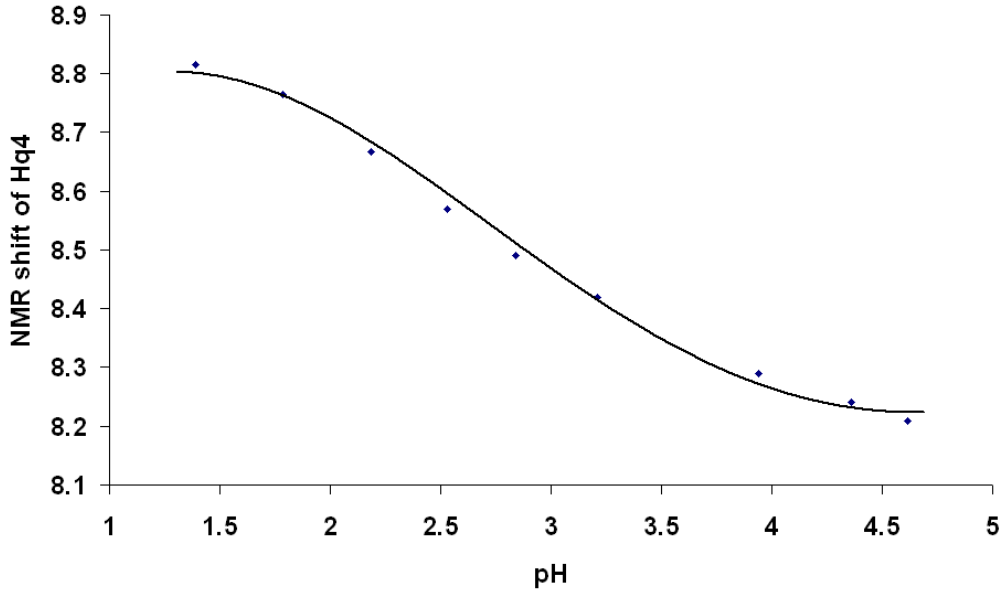

Figure-18. ^{1}H NMR shift versus pH for H_{q4} of DQPMA.

Formation Constants of DQPMA and DQPEA with Cd^{2+}

Polarographic techniques were initially employed to determine the formation constants of DQPMA and DQPEA with Zn^{2+}, Cd^{2+},Pb^{2+}, Ni^{2+}, Cu^{2+}. Only Cd^{2+} was suitable for measuring formation constants with DQPMA and DQPEA by polarography because only Cd^{2+} formed sufficiently labile systems with the two ligands.

All titrations were carried out in a background of 0.1*M* $NaNO_3$. A set of data of *E* versus volume of added DQPMA solution was collected by titration of 5.0×10^{-5} M Cd^{2+} with excess of 1.0×10^{-4} *M* DQPMA. Before any ligand was added, the standard potential of Cd^{2+}/Cd was determined from:

$$E^\circ = E - 0.05916/2 \log [Cd^{2+}]_{initial}$$

With the standard potential and the titration data, a set of values of the formation constant of Cd-DQPMA (CdL) complex could be calculated by applying the equations:

$$[Cd^{2+}] = 10^{(E - E^\circ)/\ 0.02958}$$

$$[CdL] = [Cd^{2+}]_{initial} - [Cd^{2+}]$$

$$L_{free} = (vol.L_{added} \times conc.\ L) - CdL$$

$$\log K = \log(CdL / (L_{free} \times [Cd^{2+}]))$$

where L = DQPMA.

Polarography the Cd^{2+}-DQPMA system is shown in Figure-19. Note that when the excess of DQPMA appears, the system demonstrates labile behavior.

Table-3 and Table-4 show formation constants for Cd^{2+}-DQPMA and Cd^{2+}-DQPEA. log K_1 for Cd^{2+}-DQPMA is 8.59 and that for Cd^{2+}-DQPEA is 8.03.

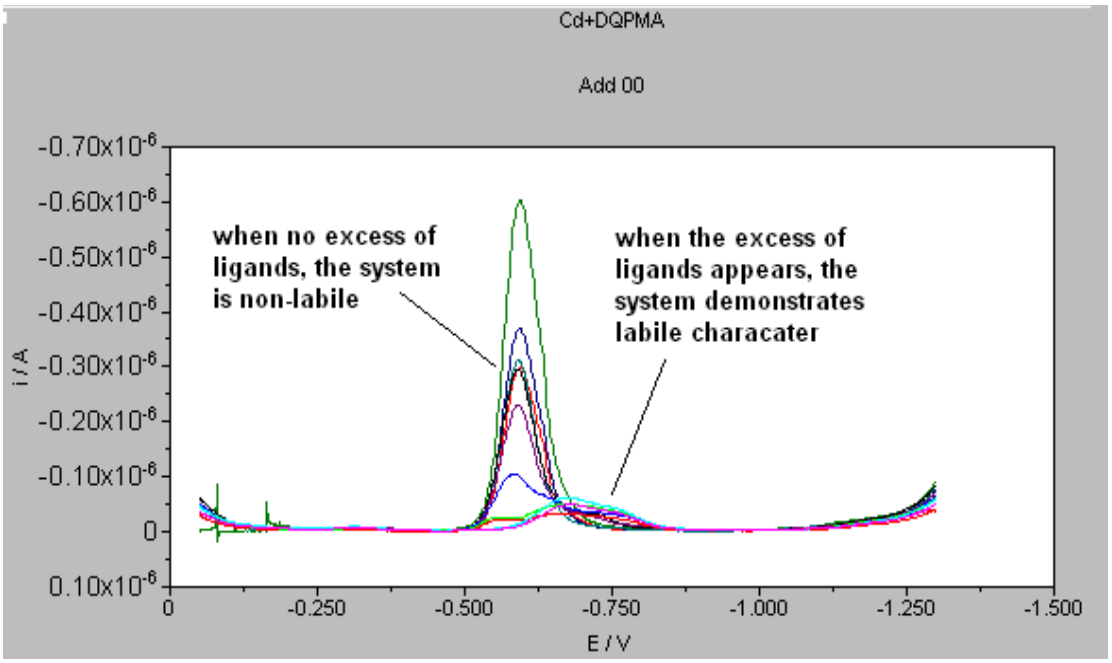

Figure-19. The polarogram of Cd^{2+}-DQPMA system.

Table-3. Determination of log *K* for Cd^{2+}-DQPMA by polaorography.

vol added	E (mv)	Cd2+	Cd total	CdL	L total	L free	logK	Aver
0	−0.584	0.00005						
27	−0.687	1.65E-08	3.247E-05	3.25E-05	3.51E-05	2.61E-06	8.88	8.59±0.15
28	−0.685	1.92E-08	3.205E-05	3.2E-05	3.59E-05	3.87E-06	8.63	
29	−0.691	1.21E-08	3.165E-05	3.16E-05	3.67E-05	5.08E-06	8.71	
30	−0.693	1.03E-08	3.125E-05	3.12E-05	3.75E-05	6.26E-06	8.68	
31	−0.691	1.21E-08	3.086E-05	3.09E-05	3.83E-05	7.42E-06	8.54	
32	−0.687	1.65E-08	3.049E-05	3.05E-05	3.9E-05	8.55E-06	8.33	
33	−0.693	1.03E-08	3.012E-05	3.01E-05	3.98E-05	9.65E-06	8.48	
34	−0.697	7.57E-09	2.976E-05	2.98E-05	4.05E-05	1.07E-05	8.56	
35	−0.693	1.03E-08	2.941E-05	2.94E-05	4.12E-05	1.18E-05	8.38	
36	−0.701	5.54E-09	2.907E-05	2.91E-05	4.19E-05	1.28E-05	8.61	
37	−0.703	4.74E-09	2.874E-05	2.87E-05	4.25E-05	1.38E-05	8.64	
38	−0.705	4.06E-09	2.841E-05	2.84E-05	4.32E-05	1.48E-05	8.68	

Titrating 40 ml 5.0×10^{-5} *M* $Cd(NO_3)_2$, 0.1 *M* $NaNO_3$ with 1.0×10^{-4} *M* DQPMA 0.1 M $NaNO_3$. When excess of DQPMA was added, the system indicates labile characteristics.

Table-4. Determination of log *K* for Cd^{2+}-DQPEA by polarography

vol added	E(mv)	free Cd^{2+}	$[Cd^{2+}]_T$	CdLe	$[Le]_T$	freeLe	log K	Ave.
0	-0.61	0.000025	0.000025					
21	-0.68	1.08E-07	1.64E-05	1.63E-05	1.72E-05	9.27E-07	8.21	
22	-0.69	4.94E-08	1.61E-05	1.61E-05	1.77E-05	1.66E-06	8.29	
23	-0.69	4.94E-08	1.59E-05	1.58E-05	1.83E-05	2.43E-06	8.12	8.03±0.17
24	-0.701	2.1E-08	1.56E-05	1.56E-05	1.88E-05	3.15E-06	8.37	
25	-0.703	1.79E-08	1.54E-05	1.54E-05	1.92E-05	3.86E-06	8.35	
26	-0.699	2.45E-08	1.52E-05	1.51E-05	1.97E-05	4.57E-06	8.13	
27	-0.699	2.45E-08	1.49E-05	1.49E-05	2.01E-05	5.25E-06	8.06	
28	-0.703	1.79E-08	1.47E-05	1.47E-05	2.06E-05	5.90E-06	8.14	
29	-0.701	2.1E-08	1.45E-05	1.45E-05	2.1E-05	6.54E-06	8.02	
30	-0.703	1.79E-08	1.43E-05	1.43E-05	2.14E-05	7.16E-06	8.05	
31	-0.705	1.54E-08	1.41E-05	1.41E-05	2.18E-05	7.76E-06	8.07	
32	-0.703	1.79E-08	1.39E-05	1.39E-05	2.22E-05	8.35E-06	7.97	
33	-0.703	1.79E-08	1.37E-05	1.37E-05	2.26E-05	8.92E-06	7.93	
34	-0.703	1.79E-08	1.35E-05	1.35E-05	2.3E-05	9.48E-06	7.90	
35	-0.705	1.54E-08	1.33E-05	1.33E-05	2.33E-05	1E-05	7.94	
36	-0.705	1.54E-08	1.32E-05	1.31E-05	2.37E-05	1.05E-05	7.91	
37	-0.705	1.54E-08	1.3E-05	1.3E-05	2.4E-05	1.11E-05	7.88	
38	-0.703	1.79E-08	1.28E-05	1.28E-05	2.44E-05	1.16E-05	7.79	
40	-0.707	1.31E-08	1.25E-05	1.25E-05	0.000025	1.25E-05	7.88	

Titration of 40ml 2.5×10^{-5} *M M* $Cd(NO_3)_2$ in 0.1*M* $NaNO_3$ with 5.0×10^{-5} *M* DQPEA in 0.1 *M* $NaNO_3$ at 25 ºC. When excess of DQPEA was added, the system displayed labile characteristics.

Formation Constants of DQPMA and DQPEA with Zn^{2+}

The attempt to determine the formation constants of DQPEA and DQPMA with Zn^{2+}, Pb^{2+}, Ni^{2+}, Cu^{2+} by polarography was unsuccessful, because these do not appear to be labile systems. The polarogram of the Cu^{2+} vs. DQPMA system is shown in Figure-20. When DQPMA was added into the Cu^{2+} solution, the Cu^{2+}/Cu peak did not move, but just got smaller until it disappeared.

An approach utilizing fluorescence was followed to overcome this problem. Fluorescence intensities for the following reaction were recorded with solutions of differing Cd(II) to Zn(II) to L ratios so as to monitor the following equilibrium:

$$CdL + Zn^{2+} = Cd^{2+} + ZnL$$

where L represents ligands DQPMA or DQPEA.

$$\text{Log } ([Cd^{2+}]\times[ZnL])/([CdL]\times[Zn^{2+}]) = \Delta\log K = \log K_{ZnL} - \log K_{CdL}$$

So that $$\log K_{ZnL} = \log K_{CdL} + \Delta\log K \qquad (8)$$

Now $\log K_{CdL}$ is known. If the concentration of Cd^{2+}, ZnL, CdL, and Zn^{2+} could be calculated, $\Delta\log K$ could be calculated, the $\log K_{ZnL}$ could be determined.

The competition experiment here is applied using the equation:

$$I = kC$$

where I is the fluorescence intensity at 375nm, k is a constant related to the path length of solution, the intensity of the excitation intensity and the fluorescent property of the fluorescent compound (which here are metal complexes of Zn^{2+}, Cd^{2+} with DQPMA or DQPEA), C is the concentration of the fluorescent compound. It means that the fluorescent intensity is proportional to the concentration of the metal complexes.

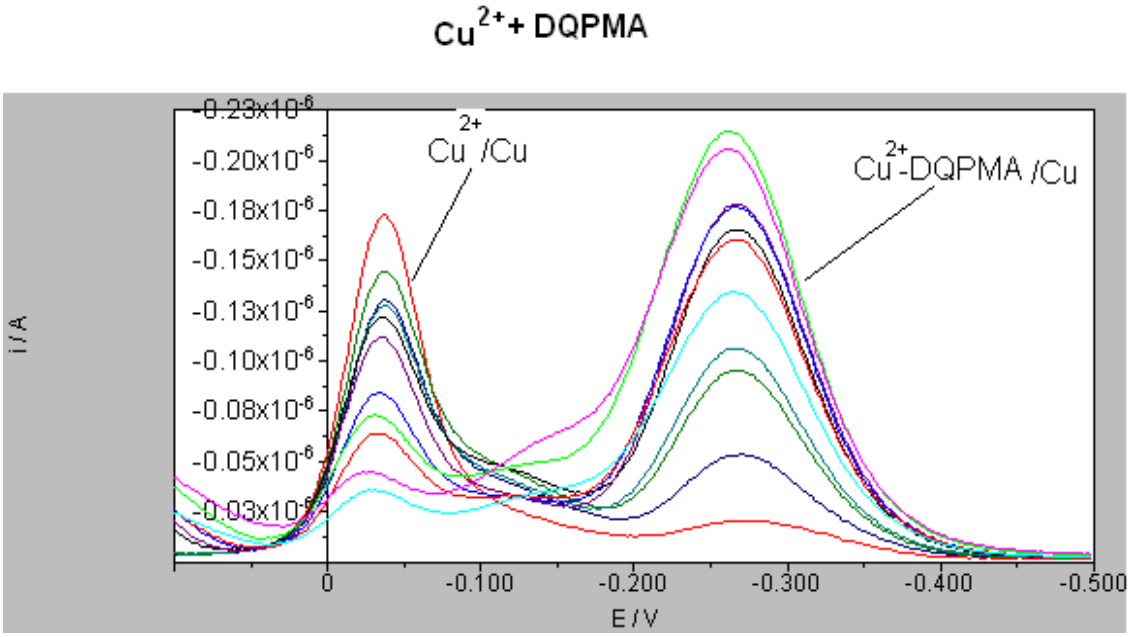

Figure-20. The polarogram of the Cu^{2+}-DQPMA system.

In the experiment, the fluorescent compound was kept constant at 10^{-4} *M*, the fluorescence intensity of the Cd^{2+}-ligand complex and Zn^{2+}-ligand complex were recorded separately at a concentration of 10^{-4} *M*. Then the fluorescence intensity of a series of the mixtures of Cd-ligand complexes and Zn-ligand complexes (the sum of the concentration of the complexes is 10^{-4} *M*) were recorded. So:

$$I_{Zn} = k_{ZnL}10^{-4} \qquad (9)$$

$$I_{Cd} = k_{CdL}10^{-4} \qquad (10)$$

$$I_{mixture} = k_{ZnL}[ZnL] + k_{CdL}[CdL] \qquad (11)$$

$$[ZnL] + [CdL] = 10^{-4} \qquad (12)$$

Where: I_{Zn} is the fluorescence intensity of Zn-ligand at 10^{-4} *M*

I_{Cd} is the fluorescence intensity of Cd-ligand at 10^{-4} *M*

k_{ZnL}, k_{CdL} are constant in Hiss law for ZnL and CdL

[ZnL], [CdL] are the concentration of ZnL and CdL in the mixtures.

So: from (9) and (11) and (12)

$$I_{Zn} - I_{mixture} = k_{ZnL}(10^{-4} - [ZnL]) - k_{CdL}[CdL]$$

$$= k_{ZnL}[CdL] - k_{CdL}[CdL]$$

$$= [CdL](k_{ZnL} - k_{CdL})$$

$$[CdL] = (I_{Zn} - I_{mixture})/(k_{ZnL} - k_{CdL}) \qquad (13)$$

from (9) and (10)

$$\Delta I = I_{Zn} - I_{Cd} = k_{ZnL}10^{-4} - k_{CdL}10^{-4} = 10^{-4}(k_{ZnL} - k_{CdL})$$

$$(k_{ZnL} - k_{CdL}) = \Delta I / 10^{-4} \qquad (14)$$

Substitute (14) into (13):

$$[CdL] = 10^{-4}(I_{Zn} - I_{mixture})/\Delta I \qquad (15)$$

Then $[ZnL] = 10^{-4} - [CdL]$

$[Zn^{2+}] = 10^{-4} - [ZnL]$

$[Cd^{2+}] = 10^{-4} - [CdL]$

Based on the calculation above, $\Delta \log K = \text{Log } ([Cd^{2+}] \times [ZnL])/([CdL] \times [Zn^{2+}])$ could be determined. Substitution of $\Delta \log K$ into (10), allows $\log K_{ZnL}$ to be determined. The fluorescence spectra of complexes of DQPMA with Zn^{2+}, Cd^{2+} at different ratios are shown in Figure-21. The fluorescent intensity data was collected from the spectral peaks.

The competition experiment between Zn^{2+} and Cd^{2+} for (a)DQPMA and for (b) DQPEA is shown in Table-5. $\Delta \text{Log} K$'s for DQPMA and DQPEA are -0.05 and 0.35 respectively:

So $\log K_{ZnLm} = 8.59 - 0.05 = 8.54$

$\log K_{ZnLe} = 8.03 + 0.35 = 8.38$

From the calculation, the conclusion can be drawn that when the size of one of the chelate rings increases from five membered to six membered, $\Delta \log K$ increases from -0.05 to 0.35 which means that the selectivity of the ligand for zinc over cadmium increases.

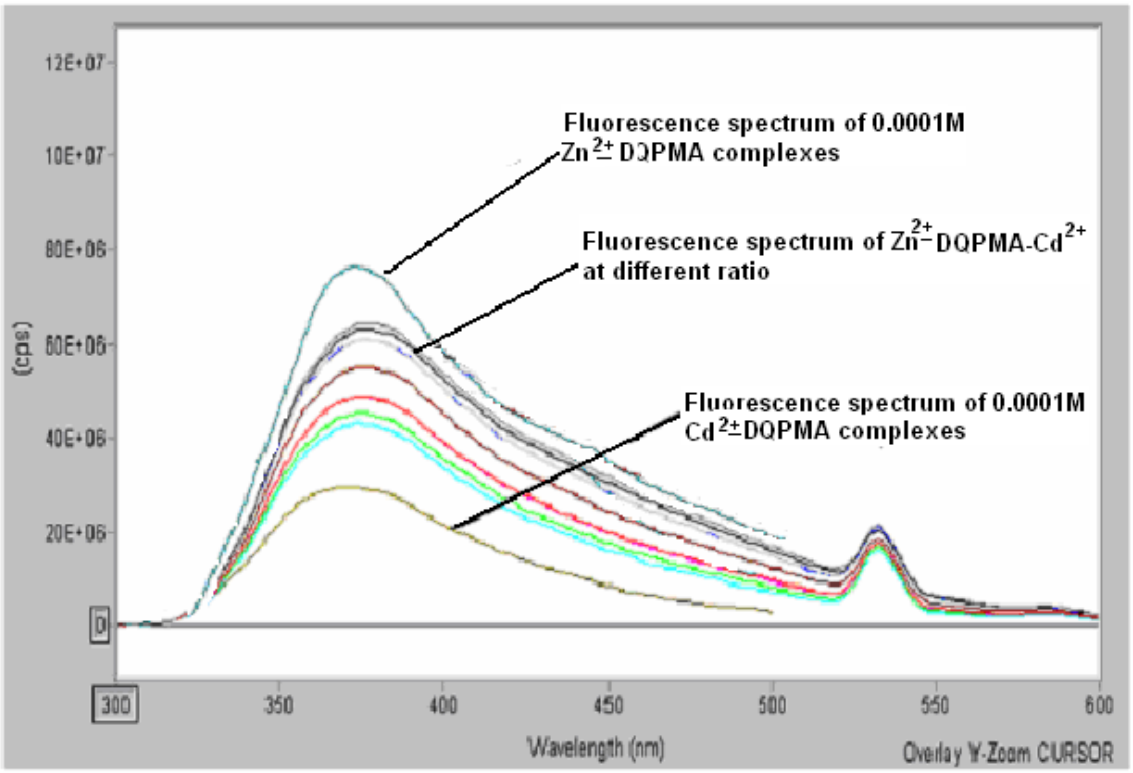

Figure-21. Fluorescence spectra of complexes of DQPMA with Zn^{2+}, Cd^{2+} at different ratios.

Table-5. Fluorescence competition experiments between Zn^{2+} and Cd^{2+} for (a) DQPMA and (b) DQPEA.

Zn:Lm:Cd	intensity	$[Zn^{2+}]_T$	$[Cd^{2+}]_T$	[ZnLm]	[CdLm]	freeZn^{2+}	freeCd^{2+}	Δ logkm	Ave.
Zn^{2+}:Lm 1:1	7.20E+7	0.0001	0	1.00E-4	0				
Cd^{2+}:Lm 1:1	3.20E+7	0	0.0001	0.00E+0	0.0001				
1:1:0.5	6.30E+7	0.0001	0.00005	7.75E-5	2.25E-5	2.25E-5	2.75E-5	-0.02	-0.05 ±0.04
1:1:1	5.50E+7	0.0001	0.0001	5.75E-5	4.25E-5	4.25E-5	5.75E-5	-0.11	
1:1:2	4.80E+7	0.0001	0.0002	4.00E-5	6.00E-5	6.00E-5	1.40E-4	-0.03	
1:1:3	4.30E+7	0.0001	0.0003	2.75E-5	7.25E-5	7.25E-5	2.28E-4	-0.06	
1:1:4	4.10E+7	0.0001	0.0004	2.25E-5	7.75E-5	7.75E-5	3.23E-4	-0.03	
0.5:1:1	5.00E+7	0.00005	0.0001	4.50E-5	5.50E-5	5.00E-6	4.50E-5	-0.13	
2:1:1	6.10E+7	0.0002	0.0001	7.25E-5	2.75E-5	1.28E-4	7.25E-5	-0.02	
3:1:1	6.30E+7	0.0003	0.0001	7.75E-5	2.25E-5	2.23E-4	7.75E-5	-0.05	
4:1:1	6.50E+7	0.0004	0.0001	8.25E-5	1.75E-5	3.18E-4	8.25E-5	-0.01	

(a)

Cd:Le:Zn	intensity	$[Cd^{2+}]_T$	$[Zn^{2+}]_T$	CdLe	ZnLe	freeCd^{2+}	freeZn^{2+}	Δ logKe	Ave.
Cd:Le 1:1	2.80E+7	0.0001	0	0.0001	0				
Zn:Le 1:1	1.30E+8	0	0.0001	0	0.0001				
1:1:1	8.80E+7	0.0001	0.0001	4.12E-5	5.88E-5	5.88E-5	4.12E-5	0.31	0.35± 0.06
2:1:1	7.30E+7	0.0002	0.0001	5.59E-5	4.41E-5	1.44E-4	5.59E-5	0.31	
3:1:1	6.40E+7	0.0003	0.0001	6.47E-5	3.53E-5	2.35E-4	6.47E-5	0.30	
4:1:1	5.90E+7	0.0004	0.0001	6.96E-5	3.04E-5	3.30E-4	6.96E-5	0.32	
1:1:2	1.10E+8	0.0001	0.0002	1.96E-5	8.04E-5	8.04E-5	1.20E-4	0.44	
1:1:3	1.15E+8	0.0001	0.0003	1.47E-5	8.53E-5	8.53E-5	2.15E-4	0.36	
1:1:4	1.20E+8	0.0001	0.0004	9.80E-6	9.02E-5	9.02E-5	3.10E-4	0.43	
5:1:0.5	4.30E+7	0.0005	0.00005	8.53E-5	1.47E-5	4.15E-4	3.53E-5	0.31	

(b)

Lm represents DQPMA, and Le represents DQPEA $[Zn^{2+}]_T$ is total Zinc, $[Cd^{2+}]_T$ is total Cadmium, $\Delta \log Km = [[ZnLm] \times [Cd^{2+}] / ([CdLm] \times [Zn^{2+}])$ for(a), $\Delta \log Ke = [[ZnLe] \times [Cd^{2+}] / ([CdLe] \times [Zn^{2+}])$

Formation Constants of DQPMA and DQPEA with Cu^{2+}

The competition experiment between Cd^{2+} and Cu^{2+} for DQPMA is shown in Table-6 and the competition experiment between Zn^{2+} and Cu^{2} for DQPEA in shown in Table-7.

For the reaction: $CdLm + Cu^{2+} = Cd^{2+} + CuLm$

$$\log K_{CuLm} = \log K_{CdLm} + \Delta \log Km$$

$$= 8.59 + 5.27 = 13.86$$

For the reaction $ZnLe + Cu^{2+} = Zn^{2+} + CuLe$

$$\log K_{CuLe} = \log K_{ZnLe} + \Delta \log Ke$$

$$= 8.38 + 5.83 = 14.21$$

Table-6. Fluorescence competition experiments between Cd^{2+} and Cu^{2+} for DQPMA.

Cu:Lm :Cd	intensity	$[Cd^{2+}]_T$	$[Cu^{2+}]_T$	CdLm	CuLm	freeCd^{2+}	freeCu^{2+}	$\Delta logKm$	Ave.
Cd:Lm1:1	2.90E+7	0.0001	0	0.0001	0				
Cu:Lm 1:1	2.80E+6	0	0.0001	0	0.0001				
1:1:10	3.00E+6	0.001	0.0001	7.63E-7	9.92E-5	0.000999	7.63E-07	5.23	5.27 ± 0.19
1:1:50	3.10E+6	0.005	0.0001	1.15E-6	9.89E-5	0.004999	1.15E-06	5.58	
1:1:100	3.50E+6	0.01	0.0001	2.67E-6	9.73E-5	0.009997	2.67E-06	5.13	
1:1:150	3.30E+6	0.015	0.0001	1.91E-6	9.81E-5	0.014998	1.91E-06	5.61	
1:1:200	3.70E+6	0.02	0.0001	3.44E-6	9.66E-5	0.019997	3.44E-06	5.21	
1:1:250	3.90E+6	0.025	0.0001	4.20E-6	9.58E-5	0.024996	4.2E-06	5.13	
1:1:300	4.00E+6	0.03	0.0001	4.58E-6	9.54E-5	0.029995	4.58E-06	5.13	
1:1:350	4.10E+6	0.035	0.0001	4.96E-6	9.50E-5	0.034995	4.96E-06	5.13	
1:1:400	4.10E+6	0.04	0.0001	4.96E-6	9.50E-5	0.039995	4.96E-06	5.19	
1:1:450	4.20E+6	0.045	0.0001	5.34E-6	9.47E-5	0.044995	5.34E-06	5.17	
1:1:500	4.20E+6	0.05	0.0001	5.34E-6	9.47E-5	0.049995	5.34E-06	5.22	
1:1:1000	4.20E+6	0.1	0.0001	5.34E-6	9.47E-5	0.099995	5.34E-06	5.52	

Lm represents DQPMA, $[Cd^{2+}]_T$ represents total Cadmium, $[Cu^{2+}]_T$ represents total Cupper, $\Delta \log Km = [[CuLm] \times [Cd^{2+}] / ([CdLm] \times [Cu^{2+}])$.

Table-7. Fluorescence competition experiments between Zn^{2+} and Cu^{2+} for DQPEA.

Zn:Le:Cu	intensity	$[Zn^{2+}]_T$	$[Cu^{2+}]_T$	ZnLe	CuLe	freeZn^{2+}	freeCu^{2+}	$\Delta \log Ke$	Ave.
Zn:Le 1:1	1.20E+08	0.0001	0	0.0001					
Cu:Le 1:1	4.00E+06	0	0.0001	0	0.0001				
600:1:1	7.30E+06	0.06	0.0001	2.84E-06	9.72E-05	0.059997	2.84E-06	5.86	5.83±0.03
650:1:1	7.50E+06	0.065	0.0001	3.02E-06	9.70E-05	0.064997	3.02E-06	5.84	
700:1:1	7.80E+06	0.07	0.0001	3.28E-06	9.67E-05	0.069997	3.28E-06	5.80	
750:1:1	7.90E+06	0.075	0.0001	3.36E-06	9.66E-05	0.074997	3.36E-06	5.81	
800:1:1	8.10E+06	0.08	0.0001	3.53E-06	9.65E-05	0.079996	3.53E-06	5.79	
850:1:1	8.10E+06	0.085	0.0001	3.53E-06	9.65E-05	0.084996	3.53E-06	5.82	
900:1:1	8.20E+06	0.09	0.0001	3.62E-06	9.64E-05	0.089996	3.62E-06	5.82	
1000:1:1	8.10E+06	0.1	0.0001	3.53E-06	9.65E-05	0.099996	3.53E-06	5.89	

Le represents DQPEA, $[Zn^{2+}]_T$ represents total Cadmium, $[Cu^{2+}]_T$ represents total Cupper, $\Delta \log Ke = [[CuLe] \times [Zn^{2+}] / ([ZnLe] \times [Cu^{2+}])$

Formation Constants of DQPMA and DQPEA with Ni^{2+}

In Table-8 are shown the competition experiments between Zn^{2+} and Ni^{2+} for (a) DQPMA and (b) DQPEA.

For the reaction: $ZnLm + Ni^{2+} = Zn^{2+} + NiLm$

$$\log K_{NiLm} = \log K_{ZnLm} + \Delta \log Km$$

$$= 8.54 - 0.63 = 7.91$$

For the reaction $ZnLe + Ni^{2+} = Zn^{2+} + NiLe$

$$\log K_{NiLe} = \log K_{ZnLe} + \Delta \log Ke$$

$$= 8.38 + 2.46 = 10.84$$

Table-8. Fluorescence competition experiments between $Zn^{2+}$and Ni^{2+} for (a) DQPMA and (b) DQPEA.

Ni:Lm:Zn	intensity	$[Zn^{2+}]_T$	$[Ni^{2+}]_T$	ZnL	NiL	free Zn^{2+}	Free Ni^{2+}	$\Delta \log Km$	Ave.
Zn:Lm 1:1	7.20E+7	0.0001	0	1.00E-4	0	0.00E+0	0		
Ni:Lm 1:1	3.70E+6	0	0.0001	0.00E+0	0.0001	0.00E+0	0		
1:1:1	5.10E+7	0.0001	0.0001	6.93E-5	3.07E-5	3.07E-5	6.93E-5	-0.71	-0.63±0.05
0.5:1:1	5.70E+7	0.0001	0.00005	7.80E-5	2.20E-5	2.20E-5	2.80E-5	-0.66	
2:1:1	4.10E+7	0.0001	0.0002	5.46E-5	4.54E-5	4.54E-5	1.55E-4	-0.61	
3:1:1	3.50E+7	0.0001	0.0003	4.58E-5	5.42E-5	5.42E-5	2.46E-4	-0.58	
4:1:1	3.30E+7	0.0001	0.0004	4.29E-5	5.71E-5	5.71E-5	3.43E-4	-0.65	
1:1:2	6.10E+7	0.0002	0.0001	8.39E-5	1.61E-5	1.16E-4	8.39E-5	-0.58	
1:1:3	6.60E+7	0.0003	0.0001	9.12E-5	8.78E-6	2.09E-4	9.12E-5	-0.66	

(a)

Ni:Le:Zn	intensity	$[Ni^{2+}]_T$	$[Zn^{2+}]_T$	ZnLe	NiLe	free Zn^{2+}	Free Ni^{2+}	$\Delta \log Ke$	Ave.
Ni:Le 1:1	9.80E+5	0.00005	0	0	0.00005	0			
Zn:Le 1:1	1.10E+8	0	0.00005	0.00005	0	0			
1:1:1	5.00E+6	0.00005	0.00005	1.84E-6	4.82E-5	4.82E-5	1.84E-6	2.83	2.46±0.21
1:1:2	7.80E+6	0.00005	0.0001	3.13E-6	4.69E-5	9.69E-5	3.13E-6	2.67	
1:1:3	1.40E+7	0.00005	0.00015	5.97E-6	4.40E-5	1.44E-4	5.97E-6	2.25	
1:1:4	1.50E+7	0.00005	0.0002	6.43E-6	4.36E-5	1.94E-4	6.43E-6	2.31	
2:1:1	1.50E+6	0.0001	0.00005	2.38E-7	4.98E-5	4.98E-5	5.02E-5	2.32	
3:1:1	1.20E+6	0.00015	0.00005	1.01E-7	4.99E-5	4.99E-5	0.0001	2.39	
4:1:2	1.10E+6	0.0002	0.00005	5.50E-8	4.99E-5	4.99E-5	1.50E-4	2.48	

(b)

Where: Lm represents DQPMA, Le represents DQPEA $[Zn^{2+}]_T$ represents total Zinc, $[Ni^{2+}]_T$ represents total Nickle, $\Delta \log Km = [[NiLm] \times [Zn^{2+}] / ([ZnLm] \times [Ni^{2+}])$
$\Delta \log Ke = [[NiLe] \times [Zn^{2+}] / (ZniLe] \times [Ni^{2+}])$

Formation Constants of DQPMA and DQPEA with Pb^{2+}

It is shown in Table-9 shows the competition experiment between Zn^{2+} and Pb^{2+} for (a) DQPMA and (b) DQPEA.

For the reaction: $ZnLm + Pb^{2+} = Zn^{2+} + PbLm$

$$\log K_{PbLm} = \log Kp_{ZnLm} + \Delta \log Km$$

$$= 8.54 - 0.83 = 7.71$$

For the reaction: $ZnLe + Pb^{2+} = Zn^{2+} + PbLe$

$$\log K_{PbLe} = \log Kp_{ZnLe} + \Delta \log Ke$$

$$= 8.38 - 2.31 = 6.07$$

Table-9. Fluorescence competition experiments between Zn^{2+} and Pb^{2+} for (a) DQPMA and (b) DQPEA.

Zn:Lm:Pb	intensity	$[Zn^{2+}]_T$	$[Pb^{2+}]_T$	ZnL	PbL	free Zn^{2+}	free Pb^{2+}	$\Delta \log Km$	Ave.
Pb:Lm 1:1	4.60E+6	0	0.0001	0	0.0001	0	0		
Zn:Lm 1:1	7.20E+7	0.0001	0	0.0001	0	0	0		
1:1:1	5.40E+7	0.0001	0.0001	7.33E-5	2.67E-5	2.67E-5	7.33E-5	-0.88	-0.83±0.04
1:1:0.5	5.90E+7	0.0001	0.00005	8.07E-5	1.93E-5	1.93E-5	3.07E-5	-0.82	
1:1:2	4.60E+7	0.0001	0.0002	6.14E-5	3.86E-5	3.86E-5	1.61E-4	-0.82	
1:1:3	4.00E+7	0.0001	0.0003	5.25E-5	4.75E-5	4.75E-5	2.53E-4	-0.77	
1:1:4	3.70E+7	0.0001	0.0004	4.81E-5	5.19E-5	5.19E-5	3.48E-4	-0.79	
2:1:1	6.50E+7	0.0002	0.0001	8.96E-5	1.04E-5	1.10E-4	8.96E-5	-0.85	
3:1:1	6.80E+7	0.0003	0.0001	9.41E-5	5.93E-6	2.06E-4	9.41E-5	-0.86	

(a)

Zn:Le:Pb	intensity	$[Zn^{2+}]_T$	$[Pb^{2+}]_T$	ZnLe	PbLe	Free Zn^{2+}	free Pb^{2+}	$\Delta \log Ke$	Ave.
Zn:Le 1:1	1.20E+08	0.0001	0	0.0001	0	0	0		
1:1:5	1.10E+08	0.0001	0.0005						
1:1:10	9.80E+07	0.0001	0.001	8.17E-05	1.83E-05	1.83E-05	0.000982	-2.38	-2.31±0.04
1:1:20	8.70E+07	0.0001	0.002	7.25E-05	2.75E-05	2.75E-05	0.001973	-2.28	
1:1:30	8.20E+07	0.0001	0.003	6.83E-05	3.17E-05	3.17E-05	0.002968	-2.31	
1:1:40	7.50E+07	0.0001	0.004	6.25E-05	3.75E-05	3.75E-05	0.003963	-2.25	
1:1:50	7.30E+07	0.0001	0.005	6.08E-05	3.92E-05	3.92E-05	0.004961	-2.29	
2:1:60	7.00E+07	0.0001	0.006	5.83E-05	4.17E-05	4.17E-05	0.005958	-2.30	
3:1:100	6.20E+07	0.0001	0.01	5.17E-05	4.83E-05	4.83E-05	0.009952	-2.34	

(b)

Where Lm represents DQPMA, Le representsDQPEA. $[Zn^{2+}]_T$ represents total Zinc ,$[Pb^{2+}]_T$ represents total lead, $\Delta\log Km = [[PbLm] \times [Zn^{2+}]/ ([ZnLm] \times [Pb^{2+}])$, $\Delta\log Ke = [[PbLe] \times [Zn^{2+}]/ ([ZnLe] \times [Pb^{2+}])$.

The formation constants of metal-ligand complexes of DQPMA and DQPEA with Ni^{2+}, Cu^{2+}, Zn^{2+}, Cd^{2+}, Pb^{2+} and the difference when one of the chelating rings changes from a five membered ring (in the case of DQPMA) to a six membered ring (in the case of DQPEA) are shown in Table-10 and Figure-22. Based on the formation constants, DQPMA has no selectivity for Zn^{2+} over Cd^{2+}, and only modest selectivity over Pb^{2+}. However DQPEA shows some selectivity for Zn^{2+} over Cd^{2+}. The principle[10,11,12] involved suggests that to increase the selectivity for a smaller metal ion such as Zn^{2+} (ionic radius r^{+} = 0.74 Å) over a larger metal ion such as Cd^{2+} (r^{+} = 0.95 Å) or Pb^{2+} (r^{+} = 1.18 Å) the size of one or more chelate rings in the ligands designed should be increased from five-membered to six-membered. This arises because, as indicated by Figure-4 and Figure-5, ligands with five-membered rings are better preorganized to complex with large metal ions, while those with six-membered rings are better preorganized to complex with small metal ions.

Table-10. Formation constants for the tripodal ligands DQPMA and DQPEA with a variety of metal ions.

Equilibrium	ionic radius of metal ions ($\overset{o}{A}$)	logK_a for		Δlog$K$
		DQPMA	DQPEA	
$Ni^{2+} + L = NiL^{2+}$	0.67	7.91	10.84	2.93
$Cu^{2+} + L = CuL^{2+}$	0.74	13.86	14.27	0.41
$Zn^{2+} + L = ZnL^{2+}$	0.74	8.54	8.38	-0.16
$Cd^{2+} + L = CdL^{2+}$	0.95	8.59	8.03	-0.56
$Pb^{2+} + L = PbL^{2+}$	1.18	7.61	6.07	-0.86

Δlog$K$ for $Le + M^{2+}Lm = M^{2+}Le + Lm$

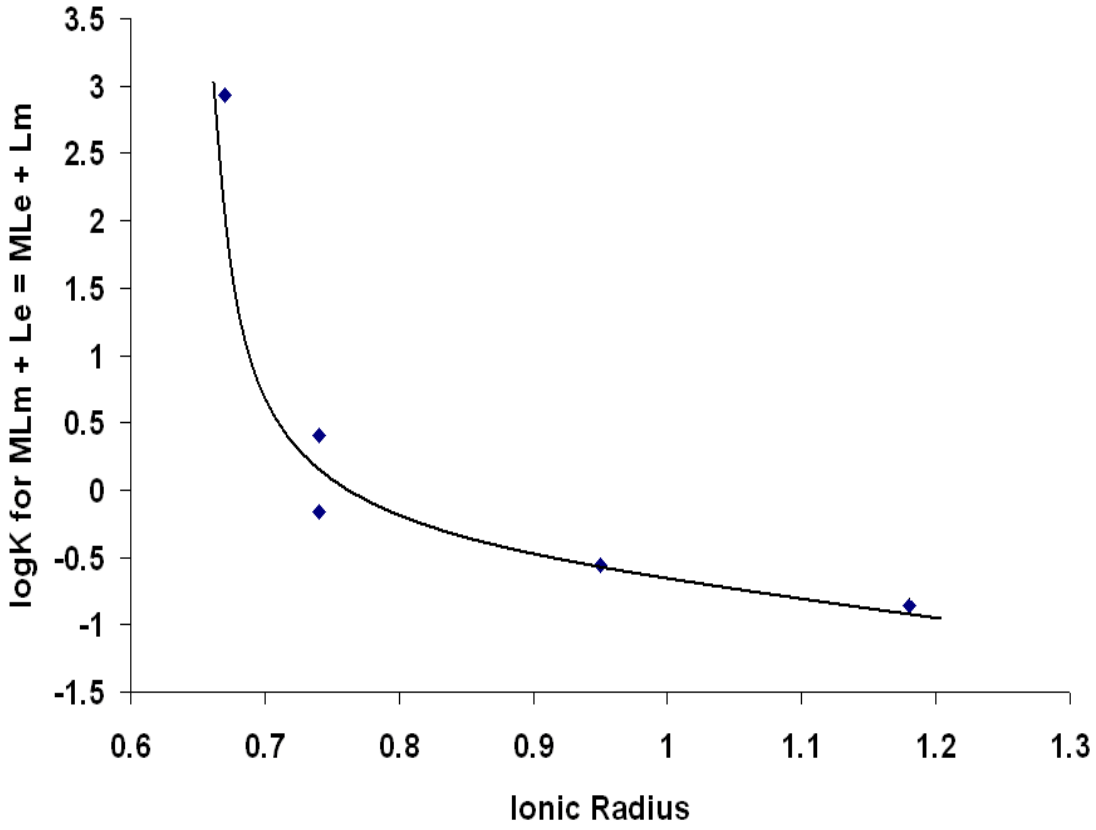

Figure-22. Ionic radii of the metal ions versus log*K* for MLm + Le = MLe + Lm where Lm represents DQPMA, and Le represents DQPEA

Analytical Methods Based on Fluorescence Properties of DQPEA

The difference in fluorescence intensity between the complexes of Zn^{2+}-DQPMA and Zn^{2+}-DQPEA at the same concentration (1.0×10^{-4} *M*) is shown in Table-11. The fluorescence intensity of Zn^{2+}-DQPEA is twice as high as that of Zn^{2+}-DQPMA. This is possibly because they have different coordination structures in aqueous solution.

The fluorescence intensity change of Zn^{2+}-DQPEA complex with changing pH is shown in Figure-23. When the pH value is less than 4, the fluorescence intensity gradually decreases because more and more DQPEA is protonated and more and more Zn^{2+}-DQPEA is broken down. When the pH drops below 2.9, no fluorescence is observed, which indicates that almost no Zn^{2+}-DQPEA is left. When the pH value is greater than 8.6, the fluorescence intensity of the complex decreases again, which indicates that the water molecule attached to the Zn^{2+} is replaced by stronger quenching ion OH^- coordinating with Zn^{2+}. With the increase in pH, some of the DQPEA is displaced by OH^- and after pH = 12, no fluorescence is observed, which shows all or most DQPEA is replaced by OH^- on the zinc. From the discussion above, it is can be concluded that the best pH range over which DQPEA can be used to detect Zn^{2+} is from pH 6.0 to 8.5.

Table-11. Fluorescence intensity of ZnLm and ZnLe.

ZnLm	Fluorescence Intensity	ZnLe	Fluorescence Intensity
10^{-4} M	7.6×10^{7}	10^{-4} M	1.3×10^{8}
5×10^{-5} M	3.7×10^{7}	5×10^{-5} M	6.5×10^{7}

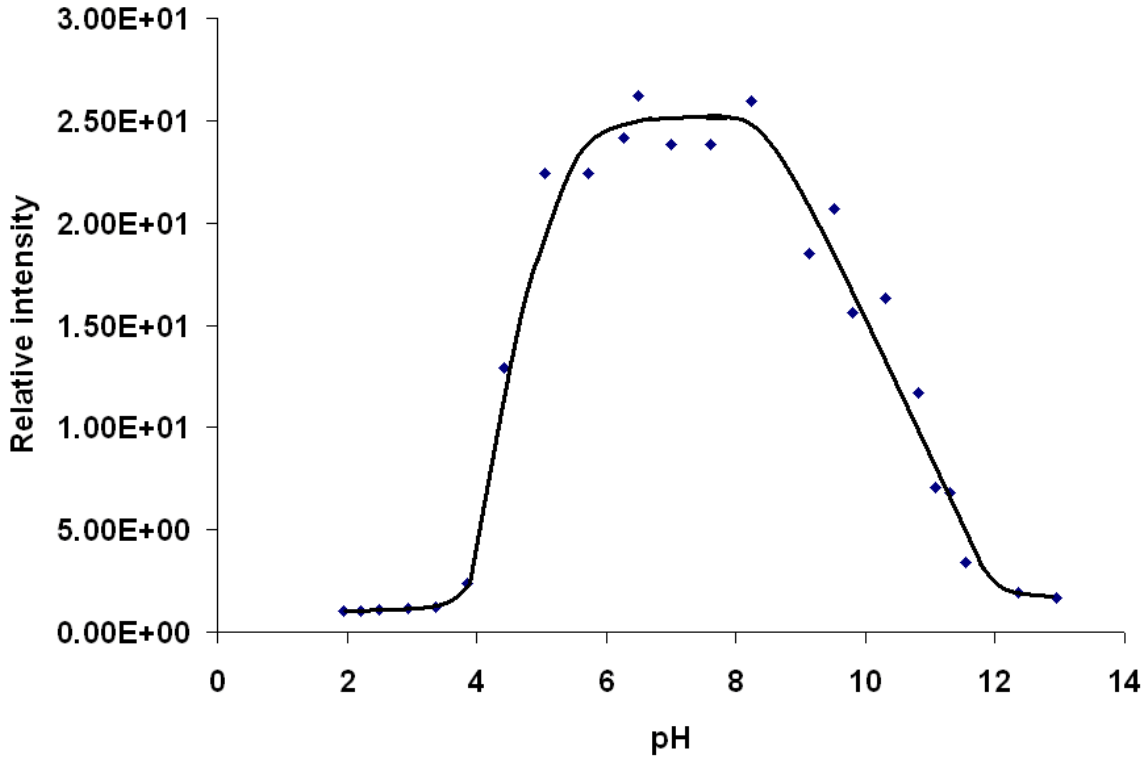

Figure-23. pH dependence of CHEF effect for Zn-DQPEA complex (5.0×10^{-5} *M*).

The change of fluorescence intensity with the change of the concentration of Zn^{2+}-DQPEA complex is shown in Figure-24. As the concentration of Zn^{2+}-DQPEA is greater than 4×10^{-6} *M*, the fluorescence property of Zn-DQPEA follows the equation:

$$I = KP_0C$$

where I is the intensity of fluorescence K is constant

P_0 is the intensity of excitation source

C is concentration of coordinate complex

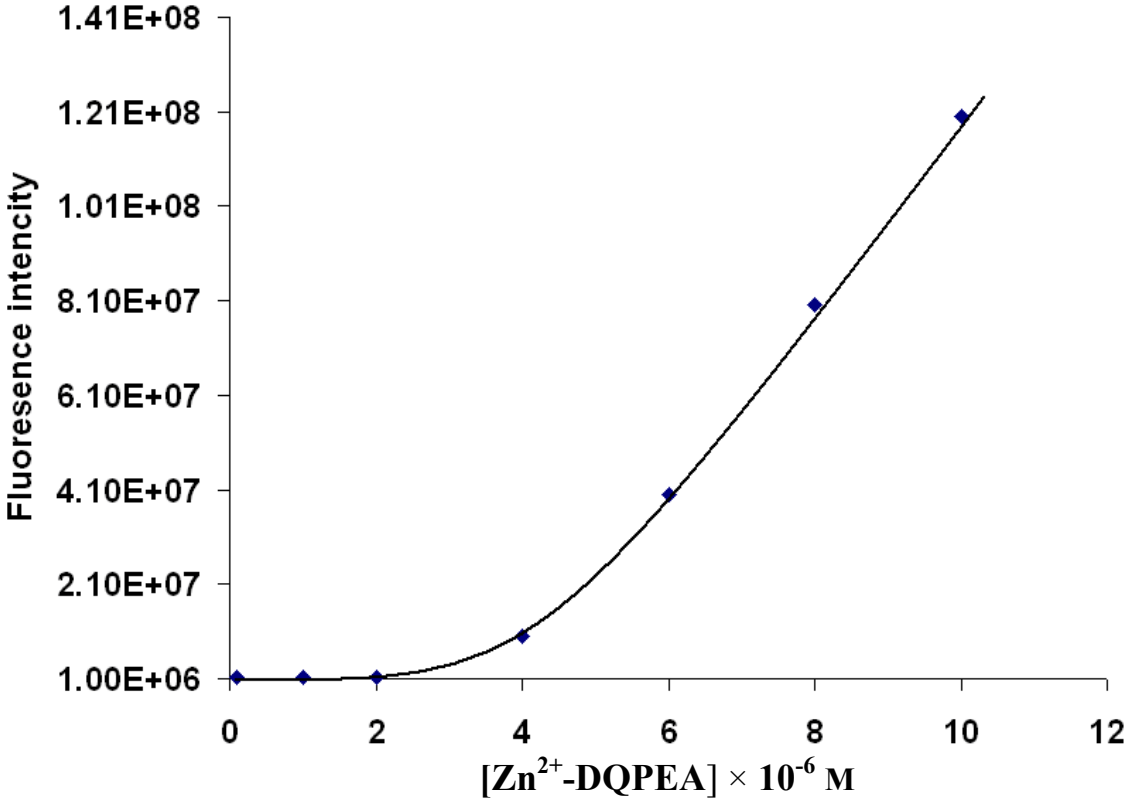

Figure-24. Fluorescence intensity versus Concentration of ZnLe at excitation wavelength of 265 nm and emission wavelength of 374 nm.

CONCLUSIONS

Based on the fluorescent properties of TQA[13] with Zn^{2+}, Cd^{2+}, Pb^{2+}, Cu^{2+}, Ni^{2+}, in order to utilize the CHEF effect to detect zinc, two ligands, DQPMA[13] and DQPEA, were synthesized to improve the solubility of the complex in water and to investigate the selectivity of the ligands for smaller versus larger ions, according to ligand design principles.[10,11,12] DQPMA and DQPEA exhibited a CHEF effect with Zn^{2+} and Cd^{2+} (Figure-8) and have much better solubility in water than TQA. DQPEA has better selectivity for Zn^{2+} over Cd^{2+} than DQPMA. Thus, increasing the size of one of the coordinating rings of the ligand from 5 (DQPMA) to six membered (DQPEA) resulted in increased selectivity for zinc over larger metal ions, and decreased selectivity of zinc versus smaller metal ions.

The properties of DQPEA still need to be improved for environmental applications. Its solubility in water is not great enough, although much better than that of TQA. The solubility of DQPEA is only 5×10^{-5} *M* in water. Additionally, upon binding Zn^{2+}, the increased fluorescence of the complex over the unbound ligand is not great enough. At less than 4×10^{-6} *M* concentration of Zn^{2+}-DQPEA complex, the fluorescence is equal to the background noise. Further investigation to increase the water solubility of the ligand and enhance the fluorescence of the metal ligand complex are necessary.